

A Computer Program For Predicting Nonlinear Uniaxial Material Responses Using Viscoplastic Models

T. Y. Chang
University of Akron
Akron, Ohio

and

R. L. Thompson
Lewis Research Center
Cleveland, Ohio

July 1984

NASA

A COMPUTER PROGRAM FOR PREDICTING NONLINEAR UNIAXIAL MATERIAL
RESPONSES USING VISCOPLASTIC MODELS

T. Y. Chang and R. L. Thompson

National Aeronautics and Space Administration
Lewis Research Center
Cleveland, Ohio 44135

SUMMARY

E-2120

A computer program was developed for predicting nonlinear uniaxial material responses using viscoplastic constitutive models. Four specific models, i.e., those due to Miller, Walker, Krieg-Swearingen-Rohde, and Robinson, are included in the present program. Any other unified model can be easily implemented into the program in the form of subroutines. Analysis features include stress-strain cycling, creep response, stress relaxation, thermomechanical fatigue loop, or any combination of these responses. In this report, an outline is given on the theoretical background of uniaxial constitutive models, analysis procedure, and numerical integration methods for solving the nonlinear constitutive equations. In addition, a discussion on the computer program implementation is also given. Finally, seven numerical examples are included to demonstrate the versatility of the computer program developed.

INTRODUCTION

The ability to perform accurate structural analysis and design studies, and ultimately durability assessments of gas turbine engine hot section components depends, to a large extent, on having good material characterization models. The material characterization for aerospace applications is made difficult because of the complex thermomechanical load history, including elevated temperatures, through which the components are cycled. The observed material deformation phenomena that result from the complex loads and that must be predicted accurately and efficiently with these models include the interaction of creep and plasticity, cyclic stress-strain hardening (or softening), rate dependence, stress relaxation, and creep recovery upon unloading. Generally, these phenomena are modelled with macroscopic (continuum) constitutive theories, which include classical plasticity theories, unified theories, decoupled theories and rheological theories. Some of these theories have been used with varying degrees of success, where each theory has its unique desirable features and modeling capabilities.

Recently, there has been considerable research effort on the development of unified theories (viscoplastic constitutive models) to predict the inelastic behavior of metals. Because the viscoplastic models can represent the interaction of creep and plasticity (an important material deformation phenomenon in engines) they have been applied to the characterization of hot section component materials (refs. 1 and 2). Classical theory of plasticity, on the other hand, cannot model this phenomenon, as discussed in reference 3. In classical theories the inelastic deformation is partitioned into independent plastic and creep terms, whereas in viscoplasticity theory it is combined into a single

inelastic strain term. Also, the other material deformation phenomena, such as cyclic hardening or softening, rate dependence and creep, can be better represented with the viscoplastic models than with the classical and other models. Consequently, a number of viscoplastic models have been proposed for more realistic representation of material deformation of turbine engine hot section components.

Viscoplastic models, like classical models and others, are not, however, without their shortcomings. Some of the shortcomings are: (a) the models have not been fully developed or adequately tested; (b) the determination of material parameters in these models is difficult since it is based largely on trial-and-error fitting of experimental data; (c) there is only a limited experimental data base available for materials used in hot section components; and (d) the associated constitutive differential equations have stiff regimes that present numerical difficulties in time-dependent analyses. To take full advantage of these models, the aforementioned deficiencies must be overcome. It is also noted that the differential equations of the viscoplastic models are highly nonlinear. Thus analytical solution of these equations, except in a few special cases, is impossible and numerical solutions are required.

In this report, a computerized analysis procedure to predict the nonlinear uniaxial stress-strain response of materials subjected to a variety of thermo-mechanical loads (simple to complex) using several viscoplastic models was developed. This procedure was incorporated into a computer program, called VPMODEL, with the following purposes in mind:

1. To compare the responses predicted by a theory with experimental data.
2. To help understand the physical phenomena represented in a particular viscoplastic model.
3. To perform parametric studies.
4. To conduct comparative studies of several viscoplastic models.
5. To investigate different numerical integration schemes.

The computer program is a modular structured code such that any viscoplastic model or numerical integration scheme can be added or deleted from the program without upsetting its overall coding organization. In addition, all computations for uniaxial responses under monotonic, cyclic, creep or stress relaxation loads, or any combination of these loads, are performed in an interactive mode with free-format input. A computer menu guides the analyst through the program, even to graphics plotting options for quick analysis of the data.

Included in this report is a section on the background of four viscoplastic models. Each model is briefly reviewed and the differential equations are presented in their uniaxial form. Also, included in other sections are discussions of the analysis procedure and various numerical integration schemes for solving the uniaxial stiff differential equations, computer implementation of these equations, and numerical examples to demonstrate the utilization of the computer program VPMODEL.

BACKGROUND

Numerous viscoplastic models have appeared in the literature. Although they differ in details, most of the models share several common features. For example, the inelastic strain rate is assumed to be a function of stress, loading history, and loading rate. Such dependence is introduced through the

use of two state variables, namely the equilibrium stress α and drag stress k . Moreover, the total strain rate is assumed to be the summation of the elastic and inelastic strain rate terms. With these assumptions, a skeletal form of viscoplastic models can be written as follows:

$$\dot{\epsilon}^I = f\left(\frac{\sigma - \alpha}{k}\right) \quad (1)$$

$$\dot{\alpha} = h_{\alpha} \dot{\epsilon}^I - \gamma_{\alpha} \quad (2)$$

$$\dot{k} = h_k \dot{\epsilon}^I - \gamma_k \quad (3)$$

where

ϵ^I = inelastic strain
 σ = applied stress
 α = equilibrium stress
 k = drag stress
 $(\dot{\cdot})$ = time derivative

h_{α} , h_k and γ_{α} , γ_k are the work-hardening and recovery functions respectively; they are generally functions of applied stress, temperature and state variables. Equation (1) is the inelastic strain rate or flow law and equations (2) and (3) are called evolutionary equations for the state variables. In addition to the above relations, we invoke the assumption that the stress rate is proportional to the elastic strain rate by

$$\dot{\sigma} = E (\dot{\epsilon} - \dot{\epsilon}^I - \beta \dot{T}) \quad (4)$$

where E is the Young's modulus of the material; ϵ is the total strain; β is the thermal expansion coefficient; and T is the temperature.

By assigning appropriate terms in the evolutionary equations, several important deformation phenomena of metals can be simulated by the viscoplastic models. For example, by allowing the equilibrium stress α and drag stress k to vary with an increase in cumulative inelastic strain in equations (2) and (3), cyclic hardening (or softening) of hysteresis loops of the material can be modelled. The transient creep or stress relaxation phenomena are represented by the rapid growth of the state variables during the initial stage of loading. Such growth becomes saturated as the recovery terms in equations (2) and (3), the second terms, become dominant. That is, steady state creep is reached when the strain work-hardening (or softening) process is in dynamic equilibrium with the thermal recovery process. Other metallurgical phenomena, such as the effects of annealing and warm-working, can be included by introducing appropriate terms in the evolutionary equations. In addition, temperature dependence of the material can also be included by allowing the inelastic strain and state variables to change with temperature. One unique feature of the viscoplastic theory, differing from the classical plasticity theory, is that it does not involve the concept of a yield surface explicitly.

By proposing various mathematical expressions for the inelastic strain and state variables, a number of viscoplastic models have emerged in the literature. The more notable models are those due to Hart (ref. 4), Miller (ref. 5),

Walker (ref. 6), Krieg, Swearingen and Rohde (ref. 7), and Robinson (ref. 8). Since the Hart model can be considered as a special case of Walker's, it will not be discussed herein. In this section, only the latter four models are briefly outlined in their uniaxial differential forms.

Miller's Model

The inelastic strain rate for Miller's model was assumed to be a hyperbolic sine function of the applied stress and two state variables. The rate equations for inelastic strain and the two state variables for Miller's improved model (ref. 9) are¹

$$\dot{\epsilon}^I = B\theta' \left\{ \sinh \left[\left(\frac{\sigma/E - \alpha}{k} \right)^{1.5} \right] \right\}^n \text{sgn}(\sigma/E - \alpha) \quad (5)$$

$$\dot{\alpha} = H_1 \dot{\epsilon}^I - H_1 B \theta' [\sinh(A_1 |\alpha|)]^n \text{sgn}(\alpha) \quad (6)$$

$$\dot{k} = H_2 \left[C_2 + |\alpha| - \frac{A_2}{A_1} \cdot k^{1.5} \right] |\dot{\epsilon}^I| \text{Min}(1.0, \theta''/\theta') - H_2 C_2 B \theta'' [\sinh(A_2 k^{1.5})]^n \quad (7)$$

where

$$H_1 = H_1' \exp[-H_3 \alpha \text{sgn}(\dot{\epsilon}^I)] \quad (8)$$

$$\theta' = \exp \{ (-Q^*/RT_t) \cdot \ln(T_t/T) + 1 \} \quad \text{if } T \leq T_t \quad (9)$$

$$\theta' = \exp(-Q^*/RT) \quad \text{if } T \geq T_t \quad (10)$$

$$\theta'' = X'' \exp \left\{ - \frac{Q_{\text{recov}}}{RT_t} \cdot [\ln(T_t/T) + 1] \right\} \quad \text{if } T \leq T_t \quad (11)$$

$$\theta'' = X'' \exp \{ -Q_{\text{recov}}/RT \} \quad \text{if } T \geq T_t \quad (12)$$

$$\text{with } X'' = \exp(R_p X') \quad (13)$$

¹Some of the terms in Miller's latest model which simulate metallurgical behavior have not been included herein.

$$Q_{\text{recov}} = Q^* [1 + (R - 1) X'] \quad (14)$$

$$X' = (1 - X)^2 \quad \text{if } X \geq 1 \quad (15)$$

$$X' = 0 \quad \text{if } X \leq 1$$

$$X = \frac{\sigma/E - \alpha}{\left(\frac{A}{2}\right)^{2/3} \left(\frac{k}{1.5}\right)} \quad (16)$$

In the above equations $B, E, n, H_1, H_2, H_3, A_1, A_2, C_2, Q^*, R_p, R_Q$ are material constants, which, except for E , are temperature independent; T_t is the transition temperature of metal. Temperature dependence of the model is introduced through the use of factors θ' and θ'' (activation energies). The model considers both kinematic and isotropic hardening of the material due to the growth laws for α and k . In the original Miller's model (ref. 5), the equilibrium stress was assumed to harden linearly with inelastic strain. This circumscribes a tri-linear curve in modeling cyclic stress-strain response. The model was subsequently modified (ref. 9) to accommodate nonlinear hardening effects by allowing the constant H_1 to vary with α according to equation (8).

Walker's Model

This model was derived from a three 3-element mechanical model for viscoplastic materials (ref. 6). In its mathematical form, the inelastic strain is expressed by a power law in terms of the applied stress and two state variables. The equations for the inelastic strain rate and the rate dependent state variables are

$$\dot{\epsilon}^I = \frac{|\sigma - \alpha|^n}{k^n} \text{sgn}(\sigma - \alpha) \quad (17)$$

$$\dot{\alpha} = (n_1 + n_2) \dot{\epsilon}^I - (\alpha - \alpha_0 - n_1 \epsilon^I) \{ (n_3 + n_4 e^{-n_5 |\epsilon^I|}) |\dot{\epsilon}^I| + n_6 |\alpha|^{m-1} \} \quad (18)$$

$$k = k_1 - k_2 e^{-n_7 |\dot{\epsilon}^I|} \quad (19)$$

In the above equations there are nine material constants, namely m , n , n_1 , n_2 , n_3 , n_4 , n_5 , n_6 , n_7 , α_0 , k_1 and k_2 . For nonisothermal conditions, all material constants may vary with temperature. Since the model contains two state variables, i.e., equilibrium stress and drag stress, both the kinematic and isotropic hardening effects can be simulated. The growth law for equilibrium stress (eq. (18)), includes both dynamic and static thermal recovery terms; whereas only the static recovery was considered for the growth of drag stress, (eq. (19)). Walker's model was formulated in both differential and integral forms (ref. 1). Only the differential form is considered in this report.

Krieg, Swearingen and Rohde's (KSR) Model

The KSR model (ref. 7) is similar to Walker's model, since it also uses a power law to represent the inelastic strain rate. The inelastic strain rate equation is

$$\dot{\epsilon}^I = \frac{|\sigma - \alpha|^n}{k^n} \text{sgn}(\sigma - \alpha) \quad (20)$$

while the state variable rate equations are

$$\dot{\alpha} = A_1 \dot{\epsilon}^I - A_2 \alpha |\alpha| \left(e^{A_3 \alpha^2} - 1 \right) \quad (21)$$

$$\dot{k} = A_4 |\dot{\epsilon}^I| - A_5 (k - k_0)^n \quad (22)$$

The seven material constants in these equations are n , A_1 , A_2 , A_3 , A_4 , A_5 , and k_0 , which can be temperature dependent. Both the equilibrium stress and drag stress are included in the formulation (i.e., eq. (20)). The growth laws contain two terms, the linear hardening and static recovery terms. These terms produce tri-linear cyclic stress-strain curves or hysteresis loops. This behavior may be modified by assuming the constant A_3 in equation (21) to be very small. Furthermore, cyclic hardening could be modelled by letting the constants A_4 and A_5 have small values in equation (22) so that the drag stress grows slowly with deformation.

Robinson's Model

This model (ref. 8), to some extent, is also analogous to the previous ones. That is, the inelastic strain rate is assumed to be a power function of the effective stress and two state variables. The equations for the inelastic strain rate and the rate dependent state variables are

$$\dot{\epsilon}^I = A \cdot P\left(\frac{\sigma(\sigma - \alpha)}{W_1}\right) < \frac{(\sigma - \alpha)^2}{3k^2} - 1 >^n \operatorname{sgn}(\sigma - \alpha) \quad (23)$$

$$\dot{\alpha} = H|\alpha''|^{-\beta} \dot{\epsilon}^I - R|\alpha''|^{m-\beta} \operatorname{sgn}(\alpha) \quad (24)$$

$$\dot{k} = 0$$

where

$$\alpha'' = (\alpha' - \alpha_0) P\left(\frac{\sigma - \alpha}{W_2}\right) + \alpha_0 \quad (25)$$

$$\alpha' = \begin{cases} \alpha & , |\alpha| \geq 2\alpha_0 \\ \frac{\alpha^2}{4\alpha_0} + \alpha_0 & , |\alpha| < 2\alpha_0 \end{cases} \quad (26)$$

$$P(x) = \begin{cases} 1 & x > 1 \\ 1 - (1 - x)^2/2 & 0 \leq x \leq 1 \\ (1 + x)^2/2 & -1 \leq x \leq 0 \\ 0 & x < -1 \end{cases} \quad (27)$$

$$\langle x \rangle = \begin{cases} x & x > 0 \\ 0 & x \leq 0 \end{cases} \quad (28)$$

The eight material constants in these equations are A , n , k , β , m , H , α_0 and R ; W_1 and W_2 are smoothing constants to account for discontinuities in the material characterization and their values are selected by the analyst. For nonisothermal conditions, temperature dependence of the model is allowed by varying the constants A and R with temperature. In the above equations, the drag stress was assumed to be constant. Thus, the current version of Robinson's model only considers the kinematic hardening of materials for which its isotropic hardening has already become saturated. If isotropic hardening is desired, it can be easily introduced with a growth law for k in the form similar to equation (22) (KSR's model).

ANALYSIS PROCEDURE

With the uniaxial viscoplastic models outlined in the previous section, it is possible to analyze three basic types of material response. The types of response are

- (1) Monotonic or cyclic stress-strain response
- (2) Creep response
- (3) Stress relaxation

Also, any combination of the above responses can be obtained by specifying appropriate loading histories. The analysis may be performed for either isothermal or nonisothermal conditions. Caution should be given, however, to nonisothermal analysis, since the constitutive model must be properly defined for such a condition. Each of the basic response types are briefly described below.

Monotonic or Cyclic Stress-Strain Response

For viscoplastic materials, time dependency is an important consideration in the calculation of material response. As an example, for the purpose of describing the analysis procedure, consider for a given strain rate the cyclic stress-strain response of a material. In this case it is divided into several segments for the purpose of proceeding with the analysis: (a) loading; (b) unloading (or reverse loading); (c) loading again, etc. For each loading (or unloading) segment, the analyst must supply the following information to begin the analysis:

Temperature	T
Strain rate	$\dot{\epsilon}$
Time increment	Δt
Strain limit	ϵ_L

Using the strain limit, a stress limit σ_L may be supplied to terminate the analysis of a load segment. Based on this information, the following steps are used in the analysis procedure to calculate the stress and strain at any time t_{n+1} :

- Step 1. Calculate the increments of total strain and inelastic strain (assuming isothermal condition for discussion purposes) according to

$$\begin{aligned}\Delta \epsilon &= \dot{\epsilon} \cdot \Delta t \\ \Delta \epsilon^I &= \dot{\epsilon}^I \cdot \Delta t\end{aligned}\tag{29}$$

where $\dot{\epsilon}^I$ is computed from equation (1). The specific expression of $\dot{\epsilon}^I$ is obtained from whichever viscoplastic model is selected.

- Step 2. Calculate the stress rate and stress increment from

$$\begin{aligned}\dot{\sigma} &= E(\dot{\epsilon} - \dot{\epsilon}^I) \\ \Delta \sigma &= \dot{\sigma} \cdot \Delta t\end{aligned}\tag{30}$$

Step 3. Update the total stress, total strain and the state variables involved.

$$\sigma(t_{n+1}) = \sigma(t_n) + \Delta\sigma$$

$$\epsilon(t_{n+1}) = \epsilon(t_n) + \Delta\epsilon$$

$$\alpha(t_{n+1}) = \alpha(t_n) + \Delta\alpha$$

$$k(t_{n+1}) = k(t_n) + \Delta k$$

(31)

The above calculation steps are repeated until the total strain or stress reaches the specified limit.

Creep Response

Creep response is generally defined as the time-dependent deformation of a material under constant stress. In the laboratory, for example, a uniaxial stress is applied to a specimen in a two-step loading history to simulate creep. That is, the stress is increased at a constant rate to a prescribed value in a short time interval, say $[0, t_1]$, then held constant afterwards as shown in figure 1(a), where $t_1 \ll t_2$. In addition to two-step loading, creep tests may also be conducted under multiple-step loading as shown in figure 1(b) or under constant stress at any point on the loading/unloading branch of hysteresis loops (fig. 1(c)). To consider these different cases, a creep analysis can be conveniently performed by dividing its loading history into two or more segments. For example, the two-step loading shown in figure 1(a) is divided into: segment 1 - stress is increased from zero to a constant value, and segment 2 - stress is held constant. The required data the analyst must supply for each of the two load segments are

Segment 1

- (a) Temperature T
- (b) Strain Rate $\dot{\epsilon}$
- (c) Time step size Δt
- (d) Strain limit ϵ_L or stress limit σ_L

Segment 2

- (a) Temperature T
- (b) Time step size Δt
- (c) Hold time t_H

Division of the loading history for multistep or cyclic loadings can be made by repeating this procedure.

Stress Relaxation

In contrast to creep, stress relaxation is obtained by applying a constant strain to a specimen and holding this strain for an extended time period. In this case, the analyst must specify: temperature, strain rate, time increment, strain limit and hold time. The analysis procedure involved herein for two-step or multistep loadings is almost identical to that of creep analysis.

NUMERICAL INTEGRATION

In order to calculate the uniaxial response (either stress or strain) of a material using a viscoplastic theory, a system of highly nonlinear differential equations, such as those of equations (1) to (4) must be solved, by numerical integration. It is well known that these equations have "stiff" regimes and special attention is, therefore, required to solve them numerically. For example, the inelastic strain rate in equation (1) is a strong nonlinear function of the stress and the state variables α and k . That is to say, any small variation in σ , α and k can cause significant changes in

the value of $\dot{\epsilon}^I$. Similar behavior is also found in the growth laws (i.e., eqs. (2) and (3)). Therefore, a very small time step is often required to integrate these equations by numerical methods.

In this section, various methods for solving the nonlinear differential equations of viscoplastic models are discussed. The question of convergence control and possible ways of selecting the size of the time step are also considered. For the purpose of discussion, equations (1) to (3) are replaced by the following matrix expression

$$\dot{\underline{y}} = \underline{f}(\underline{y}, t) \quad (32)$$

This expression represents a system of nonlinear ordinary differential equations. Although various numerical schemes can be used to solve these equations (e.g., refs. 10 and 11), practical considerations must be given to three important issues: (a) their suitability for large scale stress analysis; (b) their solution accuracy; and (c) computer solution time. For instance, Gear's multistep method (ref. 12) was utilized effectively by Miller (ref. 13) for obtaining uniaxial viscoplastic response of Zircaloy, but the method is not suitable for incorporation into a finite element analysis due to the coupling of global degrees of freedom for multiple time steps. Moreover, the method requires an independent procedure to start-up an analysis (ref. 14).

In view of the above discussion, three simple numerical schemes were selected for the present analysis, namely the forward Euler (explicit), explicit trapezoidal and implicit trapezoidal integration schemes.

In the forward Euler integration scheme, the value of y at time t_{n+1} in equation (32) is approximated by

$$y_{n+1} = y_n + \Delta t \cdot \tilde{f}_n \quad (33)$$

where

$$y_{n+1} = y(t_{n+1})$$

$$y_n = y(t_n)$$

$$\tilde{f}_n = \tilde{f}(y_n, t_n)$$

If the above equation is employed in an analysis of the "stiff" differential equations, very small time steps must be enforced to avoid any numerical instability.

Instead of using equation (33), the value of y at time t_{n+1} may be approximated by an implicit trapezoidal rule

$$y_{n+1} = y_n + \frac{\Delta t}{2} (f_n + f_{n+1}) \quad (34)$$

where $f_{n+1} = f(y_{n+1})$. With the application of the Newton-Raphson method, equation (34) is rewritten for the i -th iteration

$$[I - \Delta t \cdot J^{(i)}] \Delta y^{(i)} = F - (y_{n+1}^{(i)} - \tilde{f}_{n+1}^{(i)}) \cdot \Delta t \quad (35)$$

where I = Identity matrix

$$J = \frac{\partial f}{\partial y} \quad (\text{A nonsymmetric Jacobian matrix})$$

$$\Delta y^{(i)} = y_{n+1}^{(i)} - y_n \quad (36)$$

$$F = y_n + \Delta t \cdot \tilde{f}_n / 2 \quad (37)$$

(Eq. (35) is also called an implicit trapezoidal scheme with iterations.) If this method is employed in an analysis, the immediate question is - how can it be determined whether the solution has converged or not? Several convergence criteria could be used for this purpose. One convenient way is to check the iterative value of Δy such that

$$e = \frac{\|\Delta y^{(i)}\|}{\|y\|} \leq \text{Tol.} \quad (38)$$

where

$\| \quad \|$ = Euclidean norm

Tol = Tolerance ratio

Presently, the above criterion is implemented into the computer program VPMODEL to determine the convergence of a solution. The implicitness of f_{n+1} in equation (34) may be removed by approximating

$$\tilde{f}_{n+1} = \tilde{f}_n + J_n \Delta y \quad (39)$$

$$J_n = \left(\frac{\partial f}{\partial y} \right)_{t=t_n} \quad (40)$$

Thus, equation (34) becomes

$$\left[I - \frac{\Delta t}{2} J_{\tilde{f}_n} \right] \Delta y = \Delta t \cdot \tilde{f}_n \quad (41)$$

The above equation is called the explicit trapezoidal scheme. These three schemes have been implemented into VPMODEL for the study of numerical efficiency.

Another concern is the selection of the time step. It is possible to estimate a time increment if the strain rate is expressed by a power law (Norton's law) of the form

$$\dot{\epsilon} = A \sigma_e^n \quad (42)$$

where A and n are material constants and

$$\sigma_e = (\sigma - \alpha)/k \quad (43)$$

When the Euler forward method is employed, a step size for obtaining a stable solution is given by (ref. 15)

$$\Delta t_s < \frac{\sigma_e}{nE\dot{\epsilon}} \quad (44)$$

where

Δt_s = Largest time step that can be used for obtaining a stable solution

and

E = Young's modulus

Obviously, the above estimate is valid only if the elastic strain rate is much smaller than the inelastic rate. If the constitutive equation for inelastic strain rate is considerably different from the Norton's power law, then an approximate relationship in the form of equation (42) can be established.

$$\dot{\epsilon} = A\sigma^n \quad (45)$$

with

$$\frac{1}{n} = \frac{d \ln \sigma}{d \ln \dot{\epsilon}} \quad (46)$$

In view of the above discussion and computer experimentation runs using VPMODEL, the following step size is suggested for high strain-rate ($\sim 10^{-2} - 10^{-6}$ /sec) monotonic or cyclic loading:

Euler forward integration scheme $\Delta t = \Delta t_s$

Trapezoidal integration with or without iterations $\Delta t = 5\Delta t_s$

For steady-state creep or stress relaxation a much larger step size may be employed.

For different types of loading, an automatic time step control is useful, first to speed-up computation time and second to reduce data storage requirements. This is done according to the following criteria:

Let

$\bar{\Delta t}$ a trial step size
 e calculated error
 e_{max} maximum error limit
 e_{min} minimum error limit
 Δt step size used for analysis

then

(a) $e > e_{max}, \quad \Delta t = \bar{\Delta t}/2$

(Δt is further halved until $e \leq e_{max}$)

(b) $e_{min} < e \leq e_{max}, \quad \Delta t = \bar{\Delta t}$

(c) $e \leq e_{min}, \quad \Delta t = 2\bar{\Delta t}$

(This process is repeated until, $e_{min} < e \leq e_{max}$.)

The definition of the error e varies depending on which integration scheme is to be used. The error is measured by

$e \sim \nabla f_n$ for the Euler scheme

and

$e \sim \nabla^2 f_n$ for the trapezoidal scheme

where $\nabla f_n = f_n - f_{n-1}$ (47)

$\nabla^2 f_n = f_n - 2f_{n-1} + f_{n-2}$ (48)

These equations hold for the backward difference approximation. In view of the above relationships, the measures for error are chosen to be

$$e = \frac{\| \nabla^2 f_n \|^2}{\| y_n \|^2} \cdot \Delta t \text{ for the Euler scheme} \quad (49)$$

$$e = \frac{\| \nabla^2 f_n \|^2}{\| y_n \|^2} \cdot \Delta t \text{ for the trapezoidal scheme} \quad (50)$$

On the other hand, if the implicit trapezoidal scheme is employed, it is more convenient to adopt the relationship given in equation (38) for the calculation of error.

COMPUTER IMPLEMENTATION

The analysis procedure described has been programmed and the four viscoplastic models discussed have been incorporated into a computer program called VPMODEL to calculate the uniaxial responses of materials. The uniaxial responses include cyclic stress-strain history, creep, stress relaxation, and any combination of these phenomena. It is important to recall that the purposes of writing this program are intended for: (a) correlating the responses predicted by a theory with experimentally measured data; (b) performing parametric studies of material constants for a particular viscoplastic model, (c) performing comparative studies of various viscoplastic models; and (d) investigating different numerical integration schemes in terms of their computational efficiency.

With the above purposes in mind, the following features are included in the program:

(1.) The viscoplastic models and integration schemes were coded (in Fortran) in separate modules so that they can be easily modified, added to or deleted from the program.

(2.) All computations are in an interactive mode, and the input data are specified in conversational form and free-field format.

(3.) Analysis results can be plotted graphically and/or printed numerically.

At present, material constants of two high temperature alloys for the specific models listed below are included in the program:

Hastelloy X - material - Miller's, Walker's and KSR's models
 2-1/4 Cr-1 Mo Steel - Robinson's model

Other material types or material/model combinations, if known, may be added to the program quite easily by the user.

The program begins with four primary decisions to be made by the user, namely

- (1) Material model selection
- (2) Material type

- (3) Integration scheme to be used
- (4) Analysis type

A menu for each of the above four items is listed in figure 2. After the user has made the selections, VPMODEL will proceed with the corresponding analysis in accordance with the analysis procedure outlined in section 3. At the end of each load segment, the user has several options to either continue the analysis, plot the results, or terminate the execution. A flow chart for the analysis of VPMODEL is shown in figure 2.

The graphics part of the program was written by using a Calcomp plotting package with the plotting device being either the Calcomp plotter or the Tektronix graphics terminal, or their equivalent. The free-field input format was coded externally so that the program does not rely on the availability of such software on a particular compiler.

EXAMPLES

To demonstrate the utility of the program VPMODEL, seven example problems are included in this section. Two alloys are considered, namely Hastelloy-X and 2-1/4 Cr-1 Mo ferretic steel. Hastelloy-X is used for jet engine combustor liners whereas the ferretic steel is a typical steam generator material for advanced nuclear reactors. The material constants of Hastelloy-X for the Miller, KSR and Walker models are given in references 1 and 2. Material constants for the ferretic steel with Robinson's model are reported in reference 8.

Cyclic Stress-Strain Response Using Walker's Model

The cyclic response of Hastelloy-X, represented by Walker's model, is considered first. In this case, the following analysis parameters were specified:

Temperature	T	= 1600° F (871° C)
Strain rate	$\dot{\epsilon}$	= 3.87 x 10 ⁻³ /sec
Strain limit	ϵ_L	= 0.006
Step size	Δt	= 0.04 sec
Integration method		= Explicit trapezoidal scheme

At first, one full cycle of load, consisting of three loading segments, was imposed as shown below

Segment 1	-	Loading	$0 \leq \epsilon \leq \epsilon_L$
Segment 2	-	Unloading	$\epsilon_L > \epsilon \geq -\epsilon_L$
Segment 3	-	Loading	$-\epsilon_L < \epsilon \leq \epsilon_L$

Corresponding to the above three loading segments, the following response curves were plotted:

- (a) Stress versus Strain (fig. 3)

- (b) Back stress versus Inelastic Strain (fig. 4)
- (c) Back stress versus Total Strain (fig. 5)

To obtain the cyclic stress-strain response of the material, another unloading segment (segment 4; $-\epsilon_L < \epsilon < \epsilon_L$) was added to the previous three segments and the response was plotted for the last two loading segments as shown in figure 6. The purpose of applying two extra loading segments is to ensure that Hastelloy-X has reached its saturated state due to cyclic hardening. Similar responses were obtained for different strain rates at the same constant temperature, i.e.,

Strain rates of $= 3.66 \times 10^{-4}$, 3.70×10^{-5} , 1.11×10^{-5} and 1.25×10^{-6} 1/sec and corresponding step sizes of $t = 0.4$ sec, 4 sec., 12 sec, 80 sec.

The above results are also shown in figure 6. These curves are almost identical to those in figure 59 of reference 1.

Stress Relaxation Test Using Walker's Model

A stress relaxation case can be obtained by imposing a constant strain history to the material concerned. The relaxation phenomenon of Hastelloy-X based on Walker's model is illustrated with the following loading condition:

Constant temperature	T	=	1600° F (871° C)
Strain rate	$\dot{\epsilon}$	=	$3.87 \times 10^{-3}/\text{sec}$
Strain limit	ϵ_L	=	0.006
Hold time	t_H	=	50 sec.
Initial step size	Δt	=	0.40 sec.

Initially, the material was subjected to one full cycle of strains, $-\epsilon_L < \epsilon < \epsilon_L$ (see fig. 7). Then it experienced stress relaxation under constant strain ($\epsilon = \epsilon_L$) with a hold time $t_H = 50$ sec at the maximum stress point as shown in figure 7. The total load history was applied in four segments:

Segment 1	-	Loading	$0 \leq \epsilon \leq \epsilon_L$
Segment 2	-	Unloading	$\epsilon_L > \epsilon \geq -\epsilon_L$
Segment 3	-	Reloading	$-\epsilon_L < \epsilon \leq \epsilon_L$
Segment 4	-	Constant Strain	$\epsilon = \epsilon_L$

The integration scheme used was the implicit trapezoid rule with variable step size for all the four load segments. The calculated stress history (or relaxation curve) is shown in figure 8, where the stress history corresponding to the first strain cycle is omitted. At the beginning of hold time, the stress value is about 37 ksi (255.3 MPa) and it reduces to 12.5 ksi (86.3 MPa) asymptotically after undergoing 50 seconds of relaxation.

Cyclic Stress-Strain Response Using Robinson's Model

The third example is to obtain cyclic stress-strain response of 2-1/4 Cr-1 Mo steel using Robinson's model. The material is subjected to uniaxial stress with the following conditions:

Constant temperature	$T = 1000^{\circ} \text{ F } (538^{\circ} \text{ C})$
Strain rate	$\dot{\epsilon} = 2.4 \times 10^{-2}/\text{hr}$
Strain limit	$\epsilon_L = 0.0032$
Step size	$\Delta t = 2 \times 10^{-5} \text{ hr}$
Integration scheme	= Explicit trapezoidal method

Initially, the uniaxial loading was applied in 3 segments: (a) loading; (b) unloading; and (c) reloading, similar to example 1. Corresponding to the above loading and unloading segments, two response curves were plotted.

- (a) Stress versus Strain (fig. 9)
- (b) Back Stress versus Inelastic Strain (fig. 10)

It is seen in figure 9 that corresponding to the same strain limit, the stress for the reloading segment is higher than the stress of the initial segment (virgin material). This phenomenon is associated with strain hardening effect portrayed by the model. The hardening effect becomes saturated after the material has undergone one full cycle of loading. Therefore, in order to obtain a stable cyclic stress-strain response, another unloading segment was added and the corresponding stress-strain plot is shown in figure 11. In addition to the strain rate of $2.4 \times 10^{-2}/\text{hr}$, two different strain rates were analyzed, i.e., 0.24×10^{-2} and $0.024 \times 10^{-2}/\text{hr}$, and the results are plotted in figure 11.

Creep Response Using Robinson's Model

To demonstrate how to obtain the creep response by using VPMODEL, we consider Robinson's model as an example. The test condition is specified as follows:

Constant temperature	$T = 1000^{\circ} \text{ F } (538^{\circ} \text{ C})$
Strain rate	$\dot{\epsilon} = 0.6 \times 10^{-3}/\text{hr}$
Stress limits	$\sigma_L = 8, 10, 11, 12.5, 15 \text{ ksi}$ (ksi = 6.9 MPa)
Hold times	$t_H = 2000, 2000, 2000, 870, 200 \text{ hr}$

Before the creep loading, a full cycle of stress, $\sigma = \pm \sigma_L$, was applied to the material so that its strain hardening became saturated. Then the stress was held constant at the maximum tensile stress point, i.e., $\sigma = \sigma_L$, for the designated hold time. In the analysis, the implicit trapezoidal scheme with variable step sizes was employed. The initial step size for all stress values was: $\Delta t = 1 \text{ hr}$, then the program computed required step size according to internally specified convergence tolerance. The calculated creep responses

(inelastic strain versus time) corresponding to the hold times are shown in figure 12. Again, the creep curves obtained from VPMODEL are identical to those generated by Robinson (ref. 8).

Comparison of Three Viscoplastic Models

In this example, the stress-strain response of Hastelloy-X material is predicted by the three different models (Walker, KSR and Miller) for the same temperature, strain rate and loading condition. For this purpose, we have considered five cases by varying the temperature and strain rate as defined in table 1. Only monotonic loading (one load segment) was imposed for each case and the stress-strain plots for all five cases are shown in figures 13 to 17. Ideally, for the same material under the same loading condition, the predicted responses from the different viscoplastic models should be the same. This is not the case according to the results shown in figures 13 to 17. If we use Walker's model as a basis for comparison, KSR model correlated with Walker's prediction quite well for $T = 1400^{\circ} \text{ F}$ (760° C), $\dot{\epsilon} = 3.87 \times 10^{-3} / \text{sec}$, whereas Miller's model under-estimates the stress after the inelastic strain is initiated as shown in figure 13. On the other hand, as shown in figures 14 and 15, for the same temperature but at intermediate or lower strain rates, Miller's model correlates more closely with Walker's model than KRS model. Similar qualitative results are shown in figures 16 and 17 for a higher temperature, $T = 1800^{\circ} \text{ F}$ (982° C).

Numerical Stability Using Walker's Model

To illustrate the numerical instability problem, a monotonic load case is considered. The stress-strain response based on Walker's model was calculated for three different step sizes using the forward Euler integration scheme, with $t = 0.08, 0.32$ and 0.40 sec. The results are shown in figure 18. It is obvious that significant numerical oscillation is seen for $t = 0.40$ sec and the oscillation diminishes as the step size is reduced. To make a further qualitative comparison of the three integration methods in VPMODEL, we consider again the same stress-strain response of Hastelloy-X using Walker's model. The problem was run by using the Euler forward, explicit and implicit trapezoidal methods (no interactions). According to the results shown in figure 19, the trapezoidal methods are far more accurate than the Euler method.

Thermomechanical Fatigue Loops

Thermomechanical fatigue loops (TMF) are defined in this study to be typical (or simulated) loading histories of turbine engine combustor liners. Under these realistic loading conditions, both mechanical load (in the form of imposed strain) and temperature are subjected to large changes as functions of time. Having accurate predictions of the stress/strain response for these loading conditions is essential in the structural integrity and durability assessments of combustor liners, particularly at the critical locations in a combustor liner (usually where fatigue occurs). To this end, research programs have been conducted to develop time-temperature dependent constitutive relationships and improve finite element structural analysis procedures (refs. 1 and 2).

Rather than using sophisticated finite element structural analysis programs for evaluation and comparison of the viscoplastic models for different TMF loop, the uniaxial stress/strain responses of Hastelloy-x can be determined from the viscoplastic models in VPMODEL. Considered herein for illustrative purposes are three TMF loops: Case 1 - Closed symmetric loop, Case 2 - Open symmetric loop, and Case 3 - Open nonsymmetric loop. With these specified strain and temperature histories, stress responses were calculated in VPMODEL with the Walker, KSR and Miller models. These examples are considered for two reasons: (1) to demonstrate the capability of VPMODEL in handling non-isothermal loadings; and (2) to compare the predicted uniaxial responses with the experimental data reported in reference 2.

For Case 1, the temperature varies sinusoidally with time from 800° to 1600° F (427° to 871° C) with a period of 1 min (see fig. 20). Plots of the corresponding strain histories (also varying in a sinusoidal form) and the strain-temperature relationship are shown in figures 21 and 22. Analysis results obtained from the three models in VPMODEL, which are identical with those from reference 2, are compared with experimental data in figures 23 to 25. It is noted that the experimental data stabilized after 2 cycles. Figure 23 shows that prediction made by Walker's model requires several cycles of loading-unloading before the response stabilizes, and the model considerably over-predicts the stress response. The prediction made by Miller's model, shown in figure 24, tends to reach the steady-state in the third cycle; however, the stress-strain response becomes almost a straight line as it approaches the steady-state condition. In other words, the hysteresis effect is erased by the effect of temperature, which is contrary to the experimental data. The prediction made by the KSR model, on the other hand, shows very good agreement with the experimental measurements as seen in figure 25.

For the case of the open symmetric loop, Case 2, the temperature history (fig. 26) is identical to that of Case 1: The strain history and strain-temperature plots are given in figures 27 and 28. Comparisons between predictions and experimental data are shown in figures 29 to 31. Both the Miller and KSR models attain the steady-state condition during the second TMF loop, while Walker's model stabilizes in the fourth cycle. Tensile yields at two locations in the loading branch of the hysteresis loops, as indicated in figures 29 and 31, were predicted by both the Walker and KSR models, while Miller's model did not reflect such an effect (see fig. 30). For this loading condition, the predictions by Walker's and Miller's models are reasonably close to the experimental data, while the KSR model over-predicted stress reduction for the reverse loading branch of the TMF loop.

The temperature and strain histories, and strain-temperature relationship for Case 3 are shown in figures 32 to 34, respectively. In this case, the temperature varies sinusoidally from 950° (510° C) and 1750° F (954° C) for 1 min with a hold time of 40 sec at the peak temperature. The strain is held constant at -0.43% for the hold-time period. Analysis results for the three models and experimental data are compared in figures 35 to 37. It is seen from these figures that in approaching the steady-state condition, the same behavior is exhibited as the previous loading case. Since the constant strain hold time corresponds to a constant temperature, theoretical predictions should show some degree of stress relaxation. This is indeed the case as seen in the stress-strain plots (figs. 35 to 37). However, the experimental data do not show the distinct stress relaxation changes as do the predictions.

Nevertheless, stress relaxation may have occurred gradually during the experiment. Miller's model predicts a larger amount of stress relaxation than the Walker and KSR models. Furthermore, Miller's model does not produce tensile yield in the tensile portion of the cycle and simply exhibits elastic behavior as shown in figure 36. Because of these two factors, the predictions due to the Walker and KSR models are slightly better than those from Miller's model for the third loading case.

CONCLUSIONS

A computer program called VPMODEL was developed to calculate the uniaxial responses of material by using four viscoplastic models, namely Miller, Walker, Krieg-Swearengen-Rohde, and Robinson models. The nonlinear uniaxial responses which can be analyzed are cyclic stress-strain, creep, stress relaxation, thermomechanical fatigue loop or any combination of these phenomena. In addition, three integration schemes, i.e., Euler forward difference, explicit and implicit trapezoidal methods with Newton-Raphson iterations, were implemented into the program for the study of numerical characteristics of the various constitutive models. Since VPMODEL was written on a modular basis, addition of any new viscoplastic model or modification of an existing model can be made without major coding effort. For this reason, the program serves as an efficient tool for development and refinement of viscoplastic models. It can also be used for understanding the physical nature of a given constitutive model as well as evaluating and comparing different viscoplastic models and numerical integration schemes for use in structural analysis for aerospace and other industry applications.

APPENDIX A - USER'S INSTRUCTION

Summary of Analysis Features

The current version of VPMODEL consists of the following analysis features:

- (a) Miller, Walker, KRS, and Robinson viscoplastic models.
- (b) Uniaxial responses for monotonic or cyclic loading, creep stress relaxation or any combination of these phenomena.
- (c) Isothermal or nonisothermal (e.g., thermal-mechanical cycling) condition.
- (d) Integration schemes including forward Euler method, explicit trapezoidal method, and implicit trapezoidal method with Newton-Raphson iteration.
- (e) Conversational data input with free-field format.
- (f) Interactive computations
- (g) Plotting capability on graphics terminal.

Nomenclature

In the conversational questions for data input to VPMODEL, several terminologies are referenced and they are described as follows:

- Execution - Each time when the user loads the VPMODEL program into computer to perform one or several analyses, it is called an 'execution'. This is also equivalent to a terminal session.
- Case - During each execution (or terminal session), the user may wish to perform one or several cases of analysis; for example, Case 1: Cyclic stress-strain response using Walker's model, Case 2: Cyclic stress-strain response using Miller's model, etc.
- Segment - Each case may consist of one or more load segments.
- Hold Time - The time period during which creep under constant stress or stress relaxation under constant strain is being exercised.
- Time Limit - The maximum time at which the analysis of a load segment terminates.
- Stress Limit- The maximum or minimum stress value (including the algebraic sign) at which the analysis of a load segment terminates.
- Strain Limit- The maximum or strain value (including the algebraic sign) at which the analysis of a load segment terminates.

Limitations

VPMODEL has several limitations that the user must be aware of:

- (a) Material constants are available only for Hastelloy-X - Walker's model, Miller's model and KSR's model and for 2-1/4 Cr-1 Mo - Steel Robinson's model.
- (b) The maximum number of data points is limited to '4000' for the variables: σ , E, ΔE , α , k, T, and t. This limitation can be removed by changing the array sizes in COMMON/STAVAR/ in the computer program.
- (c) Calcomp plotting routines or interface routines for IBM TSS/370 graphics system are required.

Instructions

Since the data input procedure for VPMODEL was written in a conversational form, no additional input instructions are necessary in order for the user to run the program. For each terminal session, the user needs only to provide the analysis data in answering those questions prompted by the program and which appear as a menu on the terminal screen. The following steps are followed in order to run the program on Lewis' IBM 370-3033.

- Step 1 Logon IBM 370-3033
- Step 2 Load the program into the system by entering 'vpmode1', a procdef which compiles the program and prepares it for execution.
- Step 3 Provide input data by answering the questions prompted and execute the program for the case being analyzed.
- Step 4 Provide input data for obtaining results (graphics, listings, hard copy, etc.)
- Step 5 Terminate the analysis (or execution) by entering '0' (for stop) from procedure menu.
- Step 6 Logoff

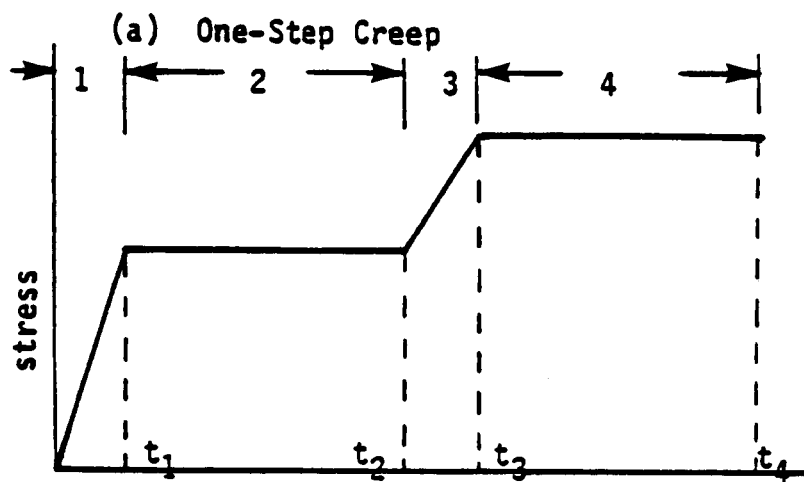
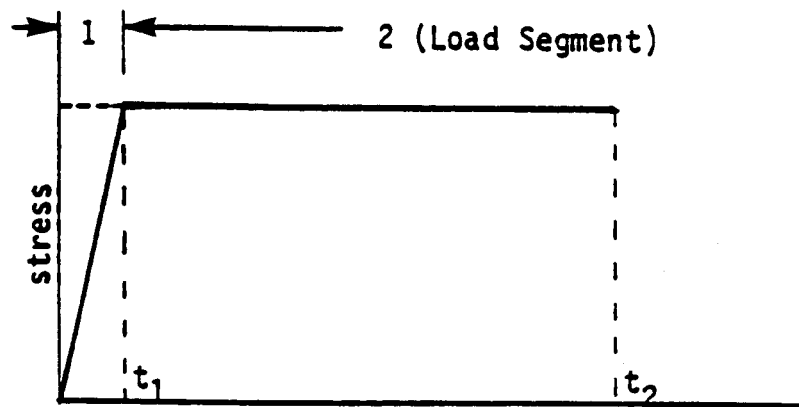
REFERENCES

1. Walker, K. P.: Research and Development Program for Nonlinear Structural Modeling with Advanced Time-Temperature Dependent Constitutive Relationships. United Technologies Research Center; (PWA-5700-50, NASA Contract NAS3-22055.) NASA CR-165533, 1981.
2. Cassenti, B. N.: Research and Development Program for the Development of Advanced Time-Temperature Dependent Constitutive Relationships. United Technologies Research Center, (R83-956077, NASA Contract NAS3-23273.) NASA CR-168191, 1983.
3. Moreno, V.: Combustor Liner Durability Analysis. Pratt & Whitney Aircraft Group, NASA (PWA-5684-19, Contract NAS3-21836.) NASA CR-165250, 1981.
4. Hart, E. W.: Constitutive Relations for the Nonelastic Deformation of Metals. J. Eng. Mater. and Technol., vol. 98, July 1976, pp. 193-202.
5. Miller, A.: An Inelastic Constitutive Model for Monotonic, Cyclic, and Creep Deformation; Parts I and II. J. Eng. Mater. Technol., vol. 98, Apr. 1976, pp. 97-113.
6. Walker, K. P.: Representation of Hastelloy-X Behavior at Elevated Temperature with a Functional Theory of Viscoplasticity. Presented at ASME/PVP Century 2 Energy Technology Conference, (San Francisco, CA.), Aug. 12-15, 1980.
7. Krieg, R. D.; Swearingen, J. C.; and Rohde, R. W.: A Physically-Based Internal Variable Model for Rate-Dependent Plasticity. Inelastic Behavior of Pressure Vessel and Piping Components, PVP-PB-028, American Society of Mechanical Engineers, 1978, pp. 15-28.
8. Robinson, D. N.: A Unified Creep-Plasticity Model for Structural Metals at High Temperatures. ORNL/TM-5969, Oak Ridge National Laboratory, 1978.
9. Miller, A. K.: Some Improvements in the "MATMOD-Z" Constitutive Equations for Nonelastic Deformation of Zircaloy, SU-DMS-82-T-1, Dept. of Materials Science and Engineering, Stanford University, 1982.
10. Krieg, R. D.: Numerical Integration of Some New Unified Plasticity-Creep Formulations. Transactions of the Fourth International Congress on Structural Mechanics in Reactor Technology, (San Francisco, Ca.), Aug 15-19, 1977, Paper No. M 6/4.
11. Kumar, V.; Morjaria, M.; and Mukherjee, S.: Numerical Integration of Some Stiff Constitutive Models of Inelastic Deformation. J. Eng. Mater. Technol., vol. 102, no. 1, Jan. 1980, pp. 92-96.
12. Gear, C. W.: The Automatic Integration of Stiff Ordinary Differential Equations. Presented at the Fourth Congress of the International Federation for Information Processing, (Edinburgh, Scotland), Aug. 5-10, 1968, pp. 281-5.

13. Sherby, O. D.: Development of the Materials Code, MATMOD (Constitutive Equations for Zircaloy). EPAI-NP-567, Electric Power Research Institute, 1977.
14. Young, D. M.; and Gregory, R. T.: A Survey of Numerical Mathematics, Vols. I and II, Addison-Wesley, 1972.
15. Corneau, I.: Numerical Stability in Quasi-Static Elastic/Viscoplasticity International Journal for Numerical Methods in Engineering vol. 9, no. 1, 1975, pp. 109-127.

TABLE I. - DIFFERENT TEST CONDITIONS FOR
MODEL COMPARISON

Case	Temperature	Strain rate	Strain limit, percent
1	1400° F (760° C)	3.87×10^{-3} /sec	0.6
2	1400° F (760° C)	3.66×10^{-4} /sec	.6
3	1400° F (760° C)	1.25×10^{-6} /sec	.6
4	1800° F (982° C)	3.87×10^{-3} /sec	.6
5	1800° F (982° C)	3.66×10^{-4} /sec	.6



(b) Two-Step Creep

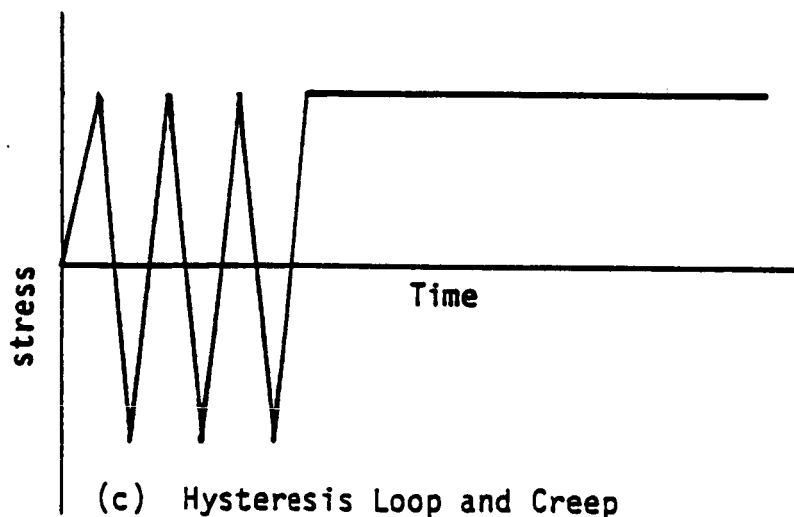


Figure 1. - Different loading histories in creep tests.

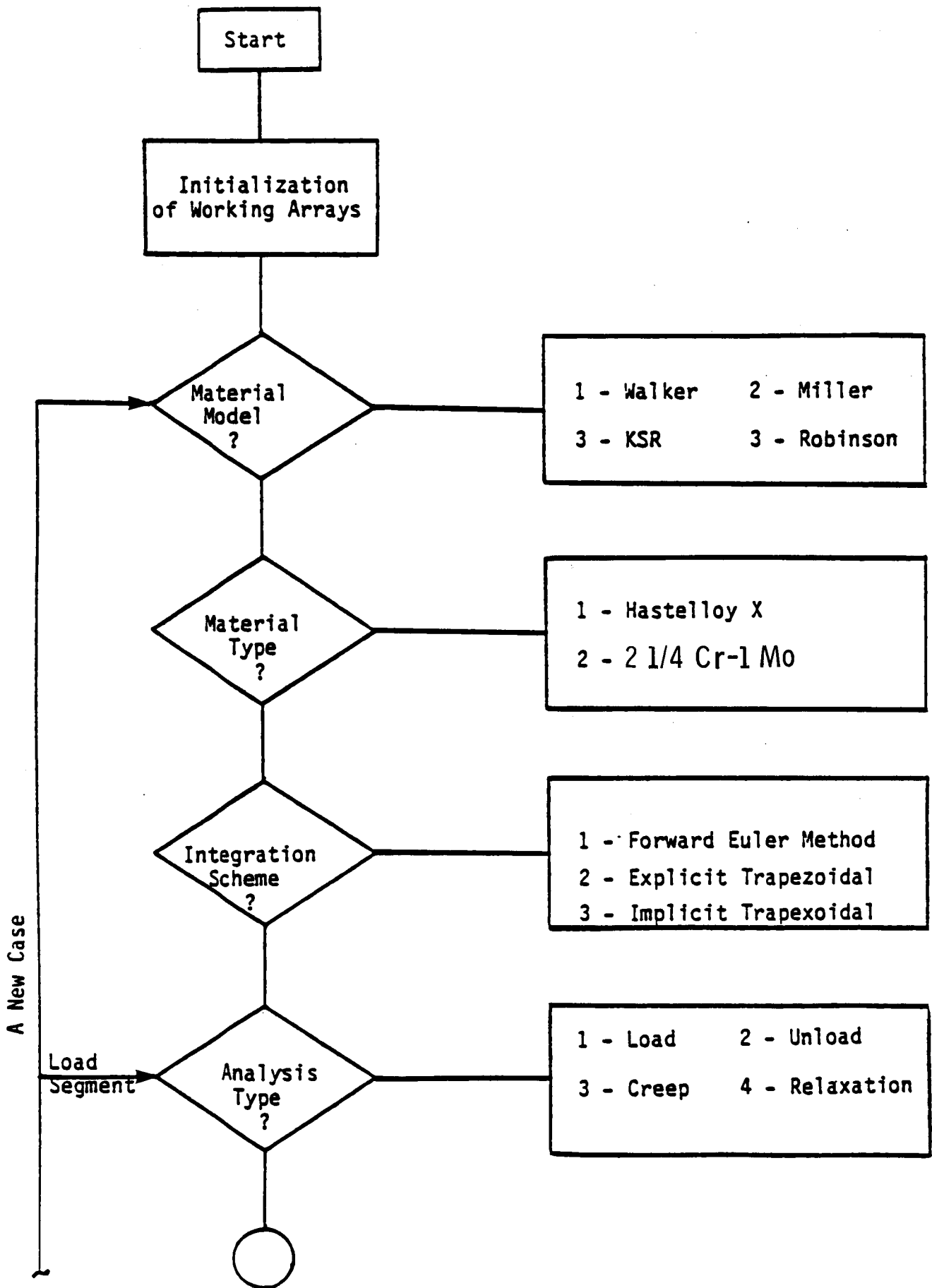


Figure 2. - A flow chart for VPMODEL.

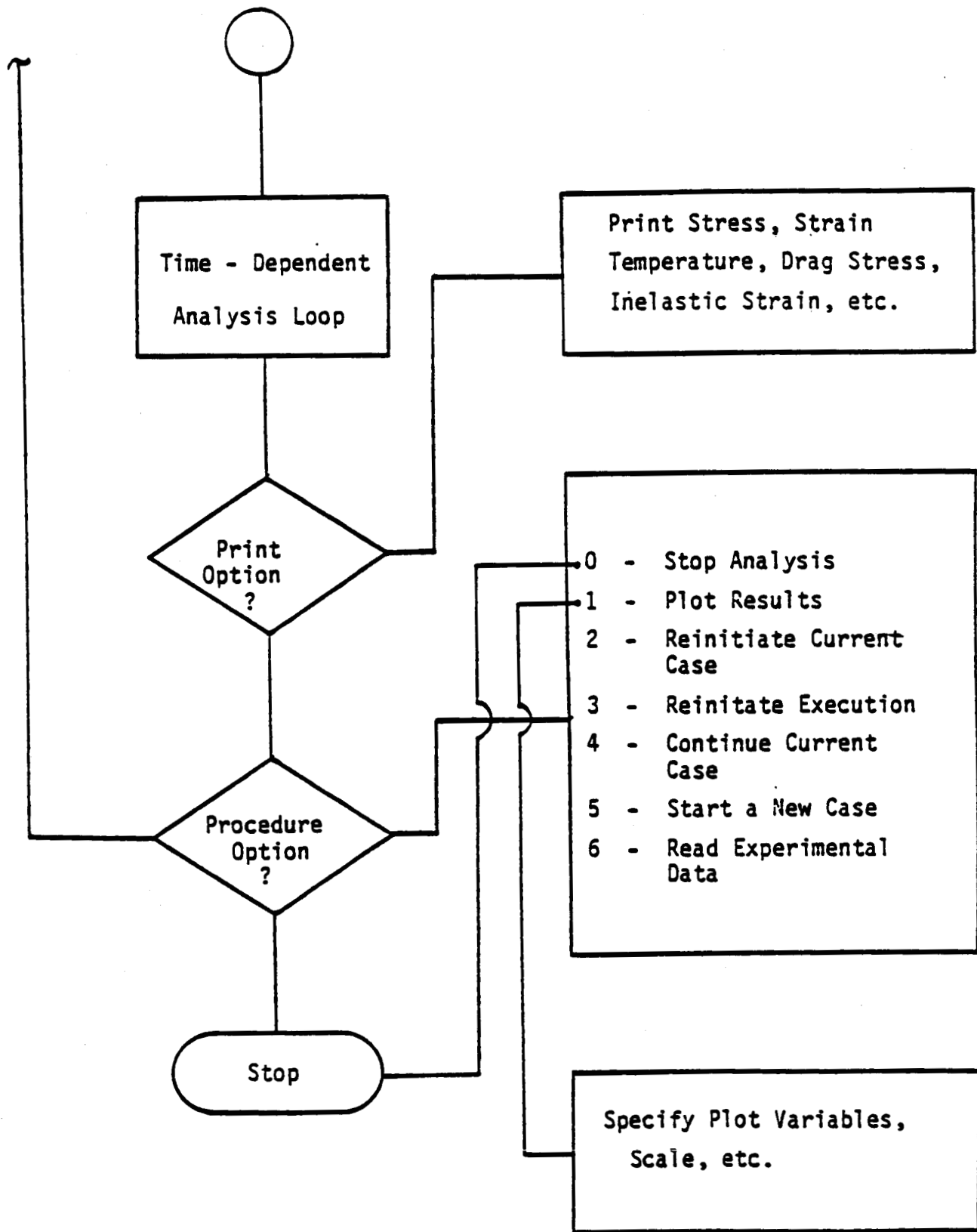


Figure 2. - Concluded.

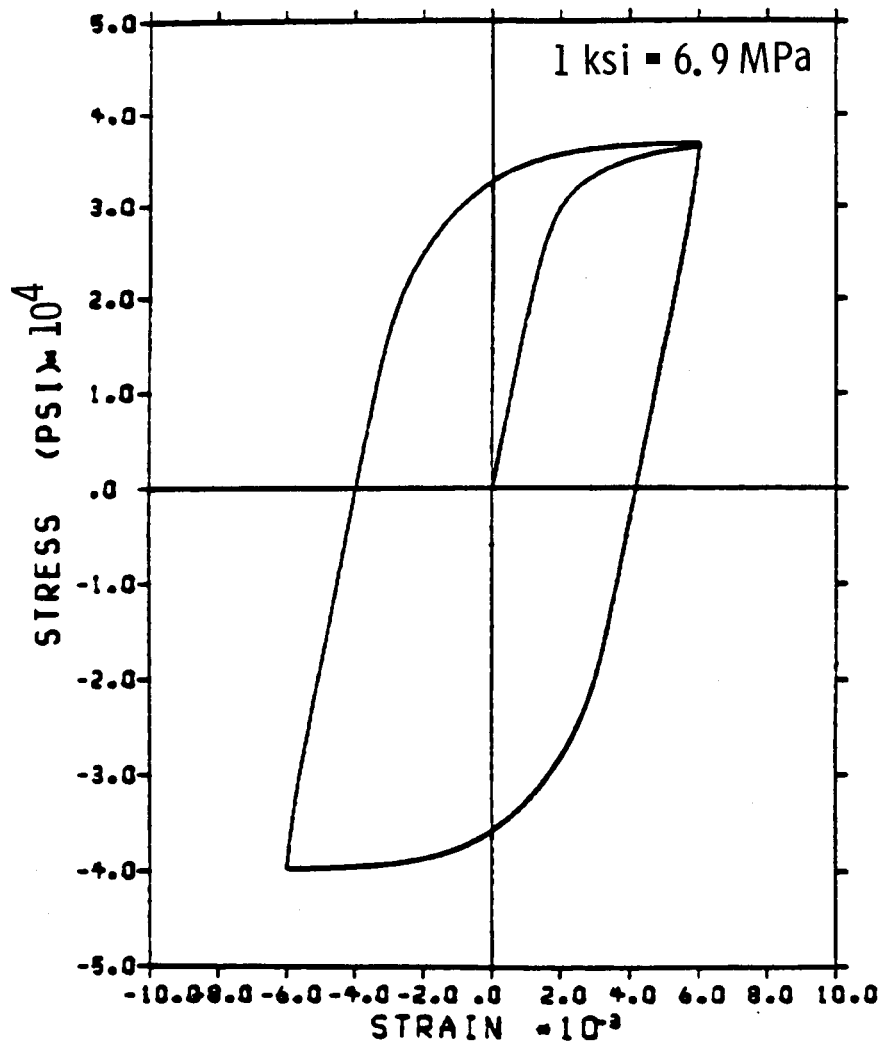


Figure 3. - Stress-strain response of Hastelloy-X, Walkers's model: $\dot{\epsilon} = 3.87 \times 10^{-3}/\text{sec}$; $T = 1600^{\circ} \text{F}$ (871°C).

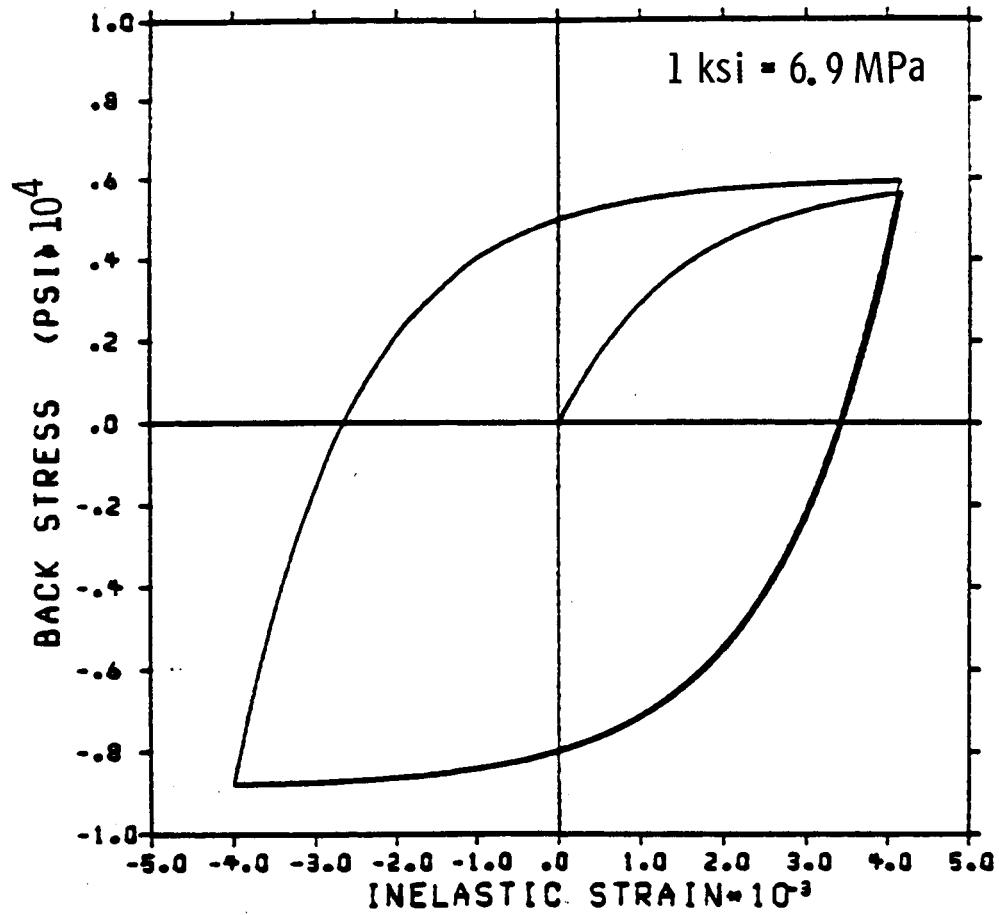


Figure 4. - Back stress vs inelastic strain for Hastelloy-X, Walker's model: $\dot{\epsilon} = 3.87 \times 10^{-3}$ / sec; $T = 1600^{\circ} \text{ F}$ (871° C).

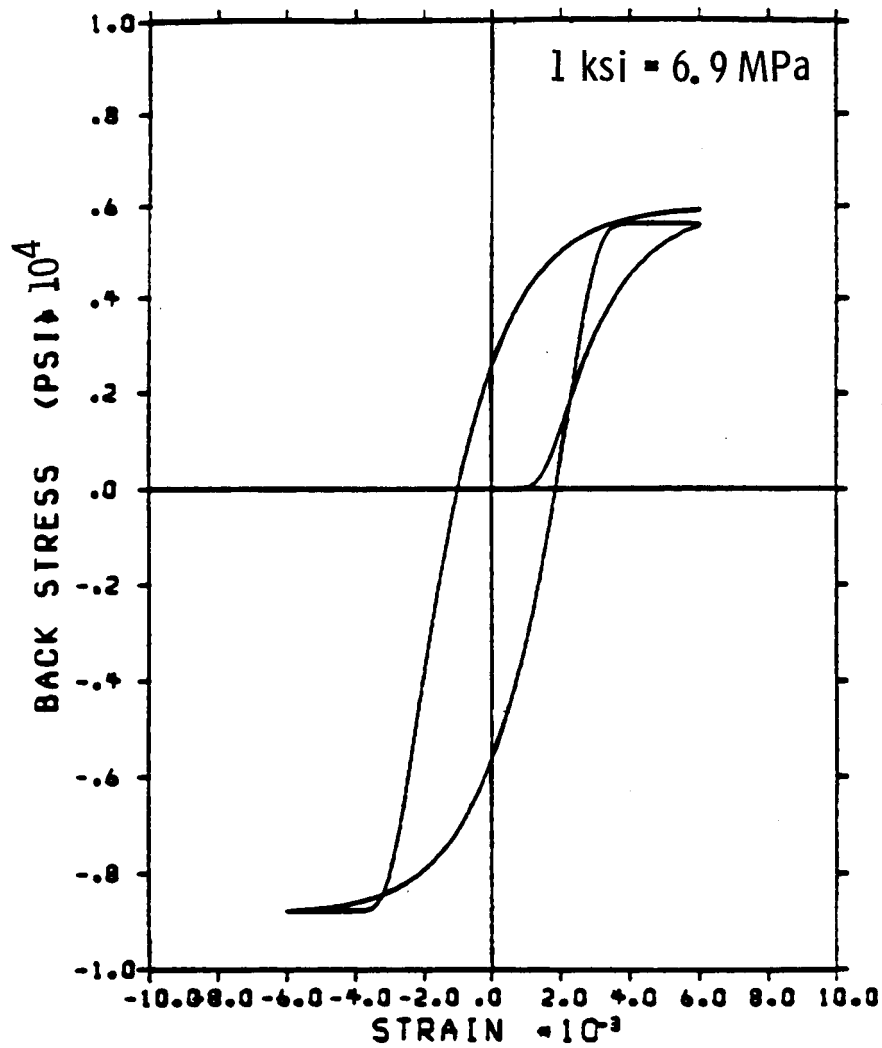


Figure 5. - Back stress vs strain for Hastelloy-X,
Walker's model: $\dot{\epsilon} = 3.87 \times 10^{-3}/\text{sec}$; $T = 1600^{\circ} \text{F}$
(871°C).

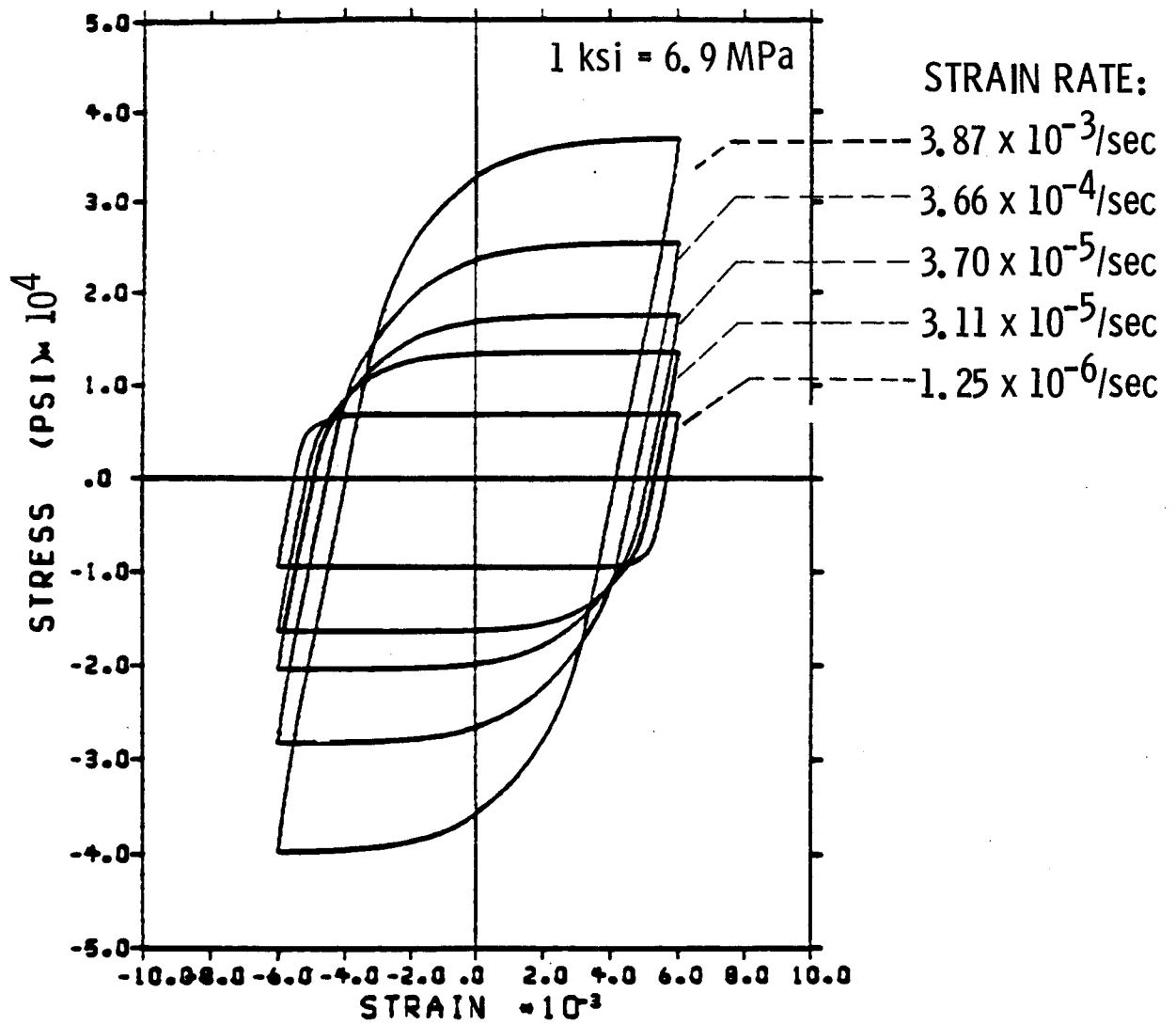


Figure 6. - Cyclic stress-strain response of Hastelloy-X, Walker's model: $T = 1600^{\circ}\text{F}$ (871°C).

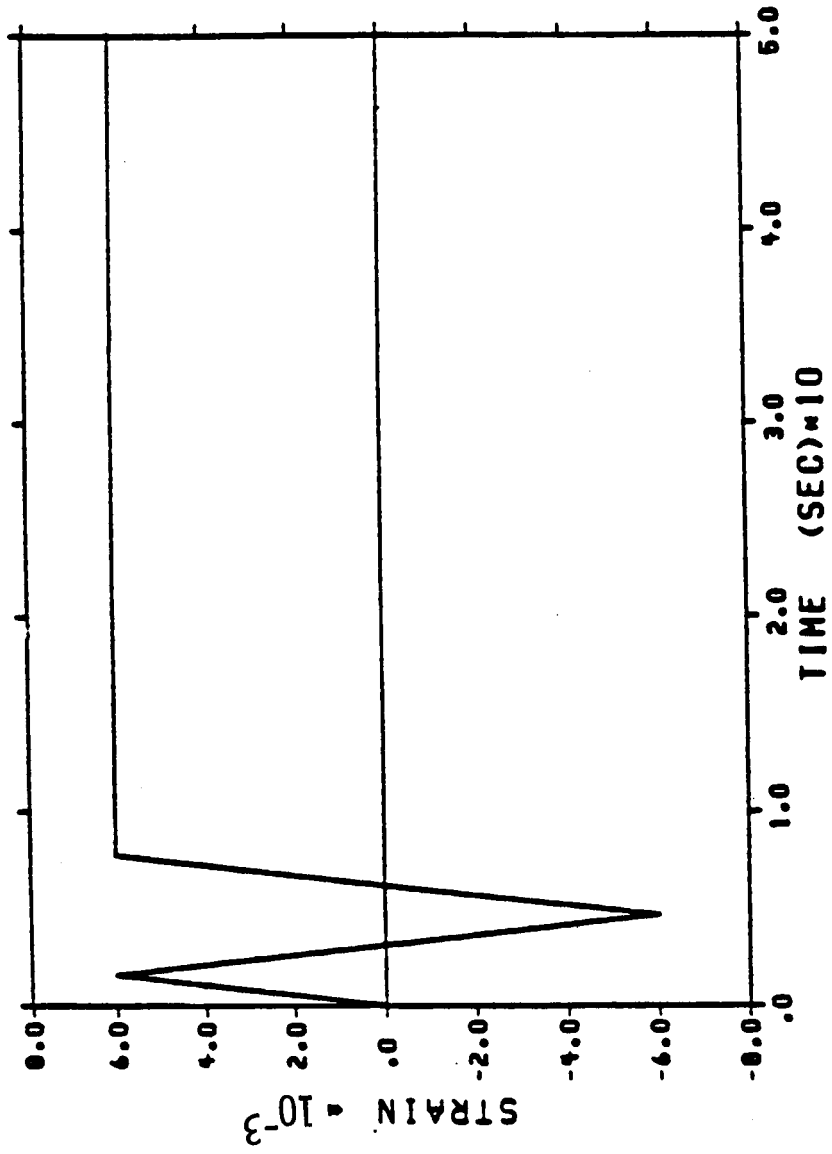


Figure 7. - Strain history for the stress relaxation test of Hastelloy-X: $T = 1600^{\circ} F$ ($871^{\circ} C$); $\dot{\epsilon} = 3.87 \times 10^{-3}/\text{sec}$.

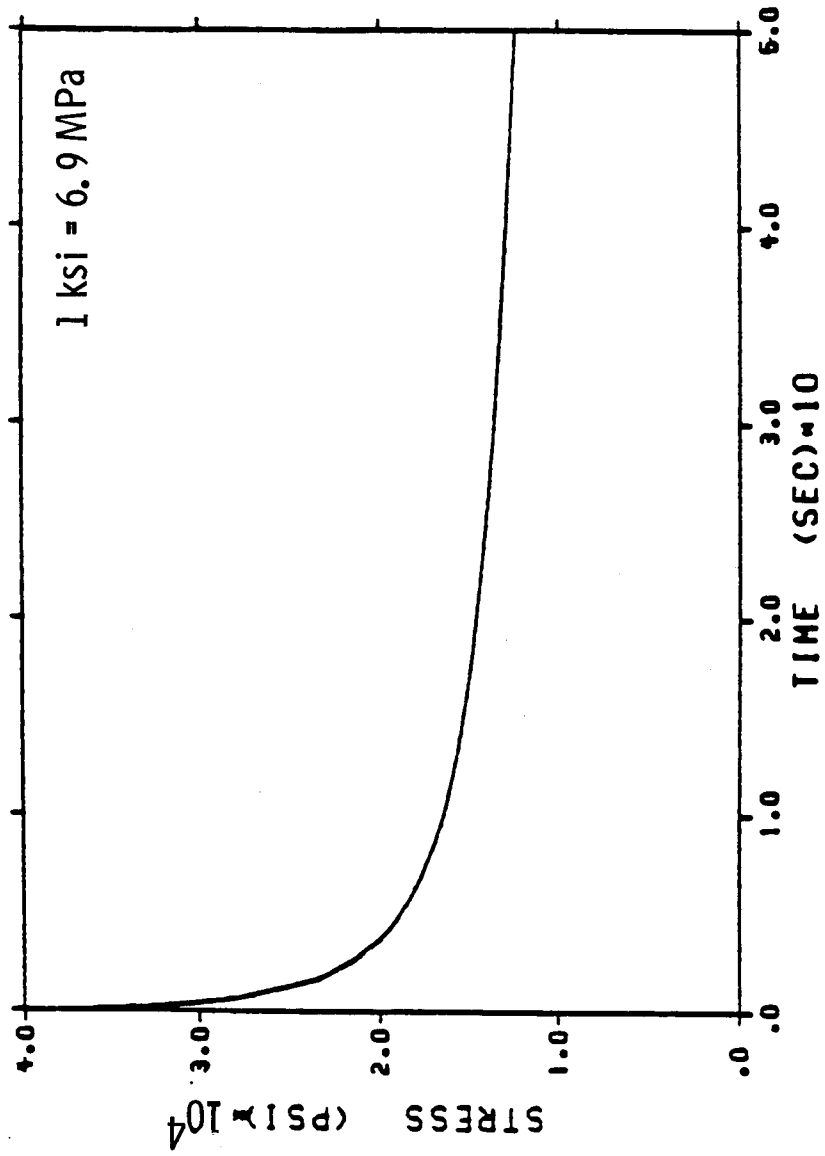


Figure 8. - Stress relaxation of Hastelloy-X, Walker's model: $\epsilon = 3.87 \times 10^{-3}$ /sec; $T = 1600^\circ \text{F}$ (871°C).

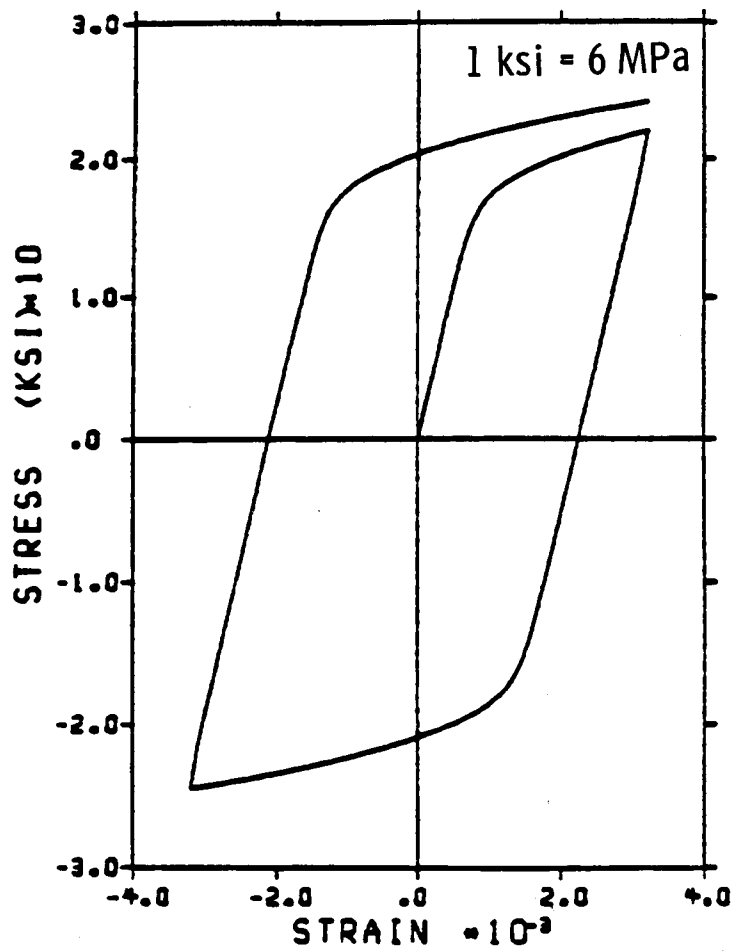


Figure 9. - Stress-strain response of 2-1/4 Cr-1 Mo steel, Robinson's model $\dot{\epsilon} = 2.4 \times 10^{-2}/\text{hr}$, $T = 1000^{\circ}\text{F}$ (538°C).

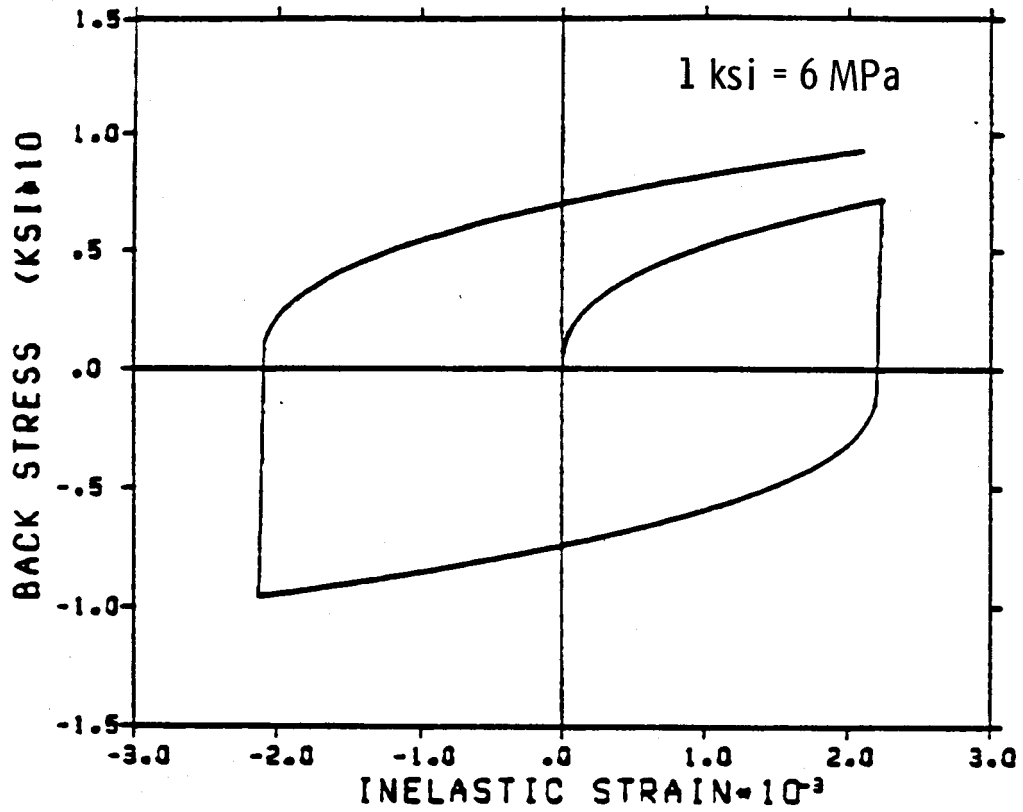


Figure 10. - Back stress vs inelastic strain, Robinson's model: $\dot{\epsilon} = 2.4 \times 10^{-2}/\text{hr}$, $T = 1000^{\circ}\text{F}$ (538°C).

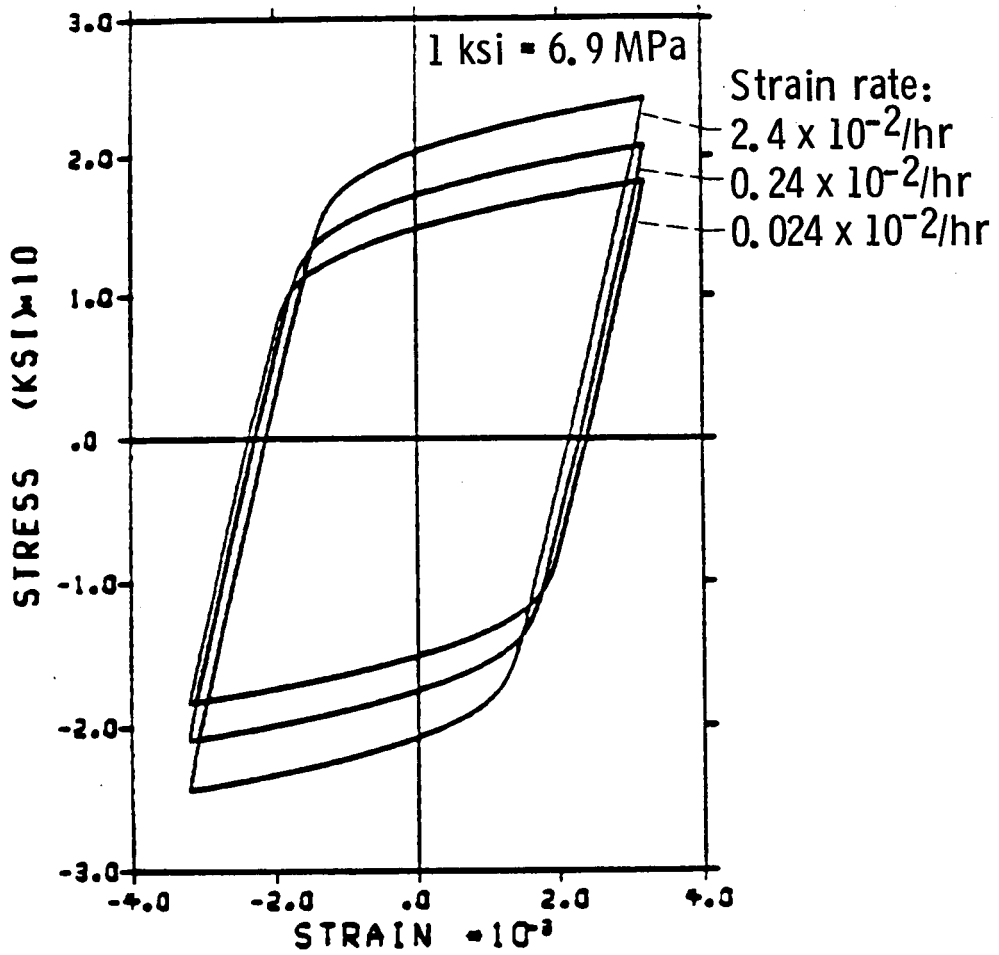


Figure 11. - Cyclic response of Robinson's model: $T = 1000^{\circ}\text{F}$ (538°C).

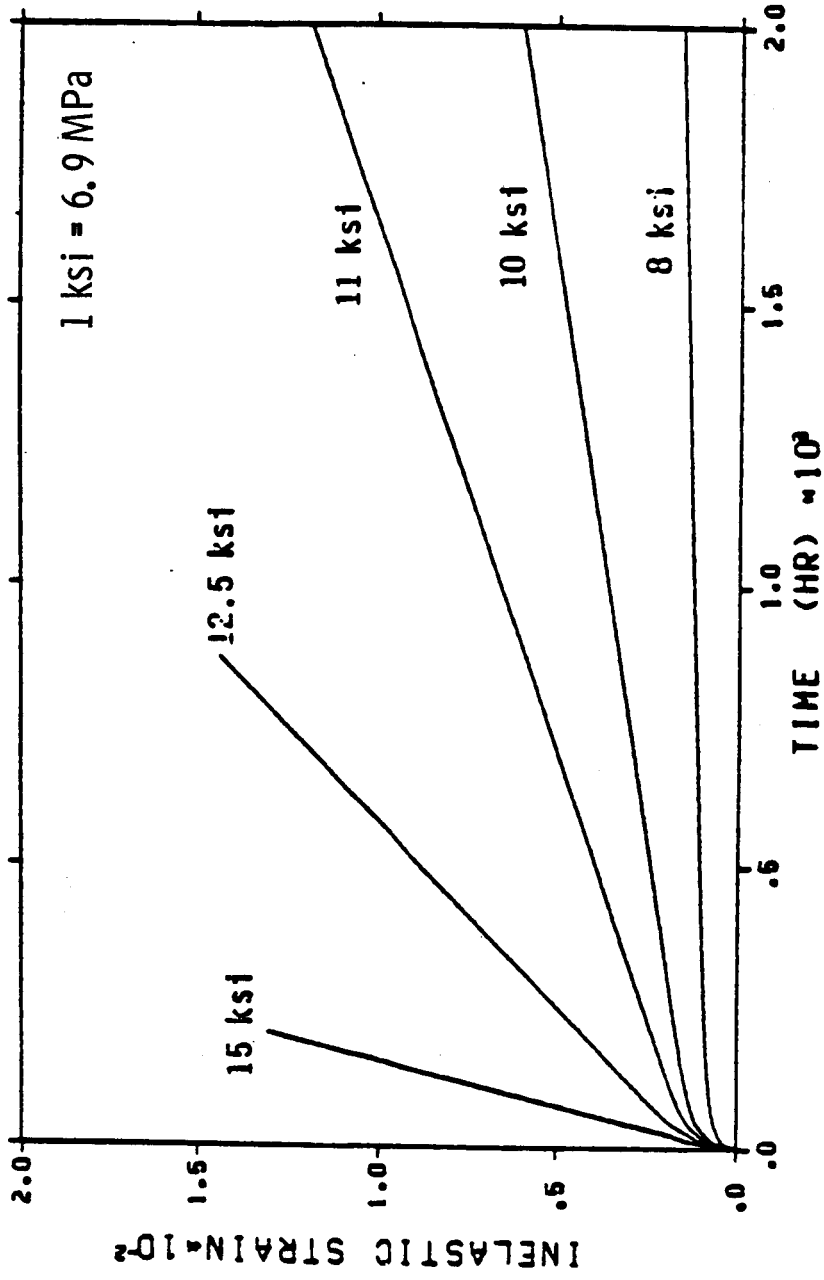


Figure 12. - Creep response of 2-1/4 Cr-1 Mo steel, Robinson's model: $\dot{\epsilon} = 0.6 \times 10^{-3}/\text{hr}$, $T = 1000^\circ \text{F}$ (538°C).

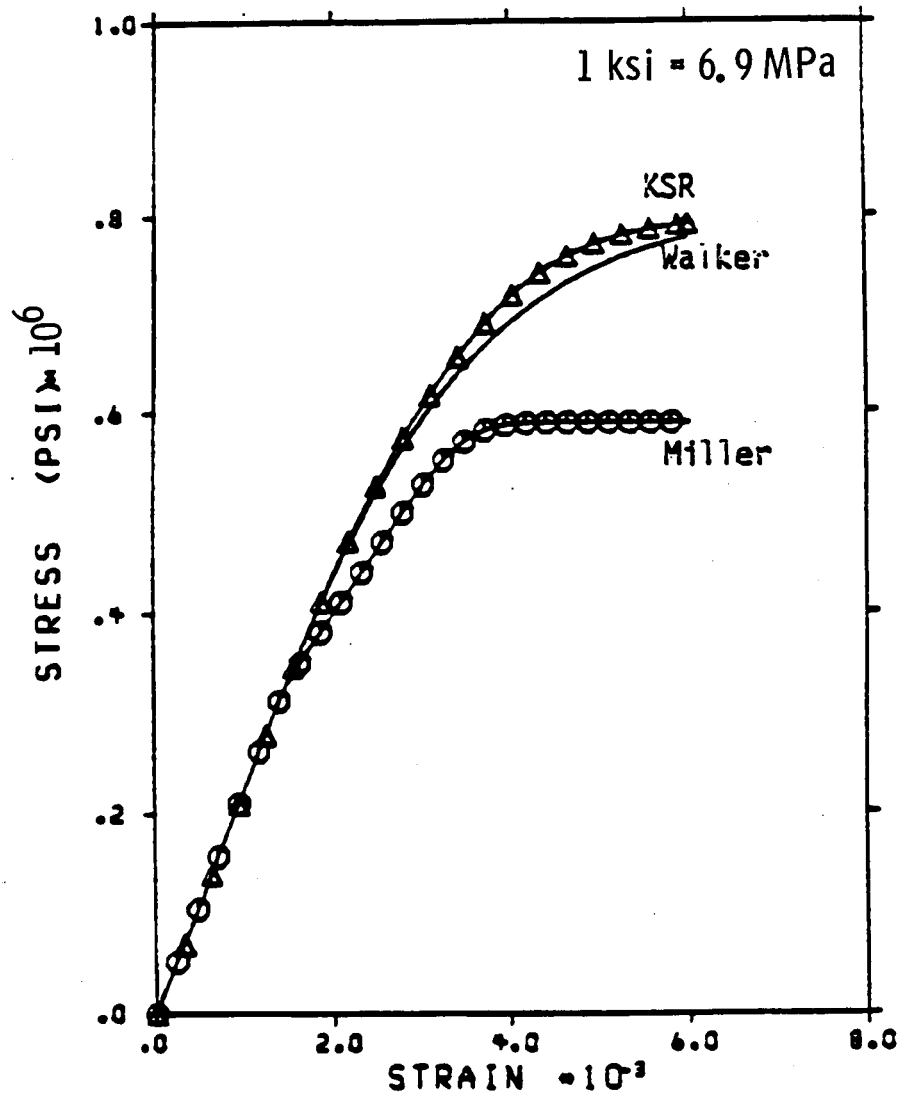


Figure 13. - Stress-strain response of Hastelloy-X: $T = 1400^{\circ} F (760^{\circ} C)$, $\dot{\epsilon} = 3.87 \times 10^{-3}/sec.$

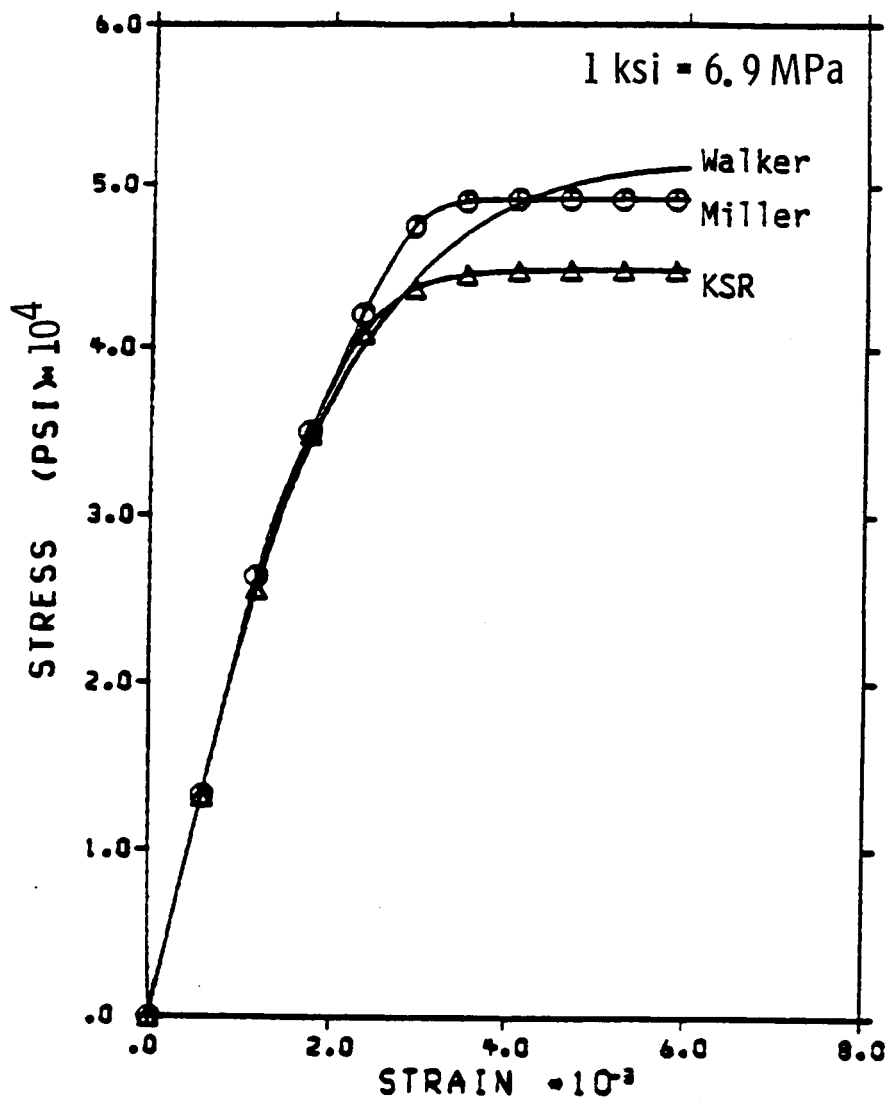


Figure 14. - Stress-strain response of Hastelloy-X: $T = 1400^{\circ} \text{F}$ (760°C), $\dot{\epsilon} = 3.66 \times 10^{-4}/\text{sec}$.

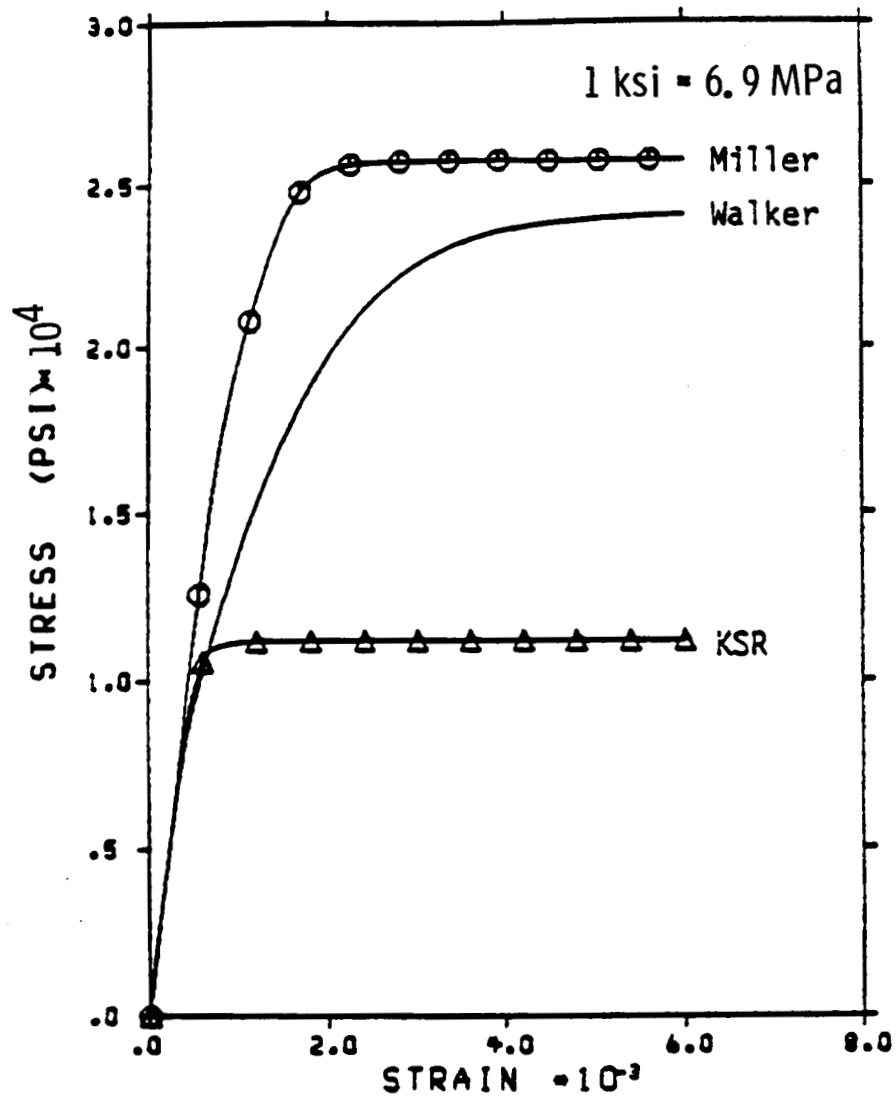


Figure 15. - Stress-strain response of Hastelloy-X; $T = 1400^{\circ}F$ ($760^{\circ}C$), $\dot{\epsilon} = 0.125 \times 10^{-5}/\text{sec}$.

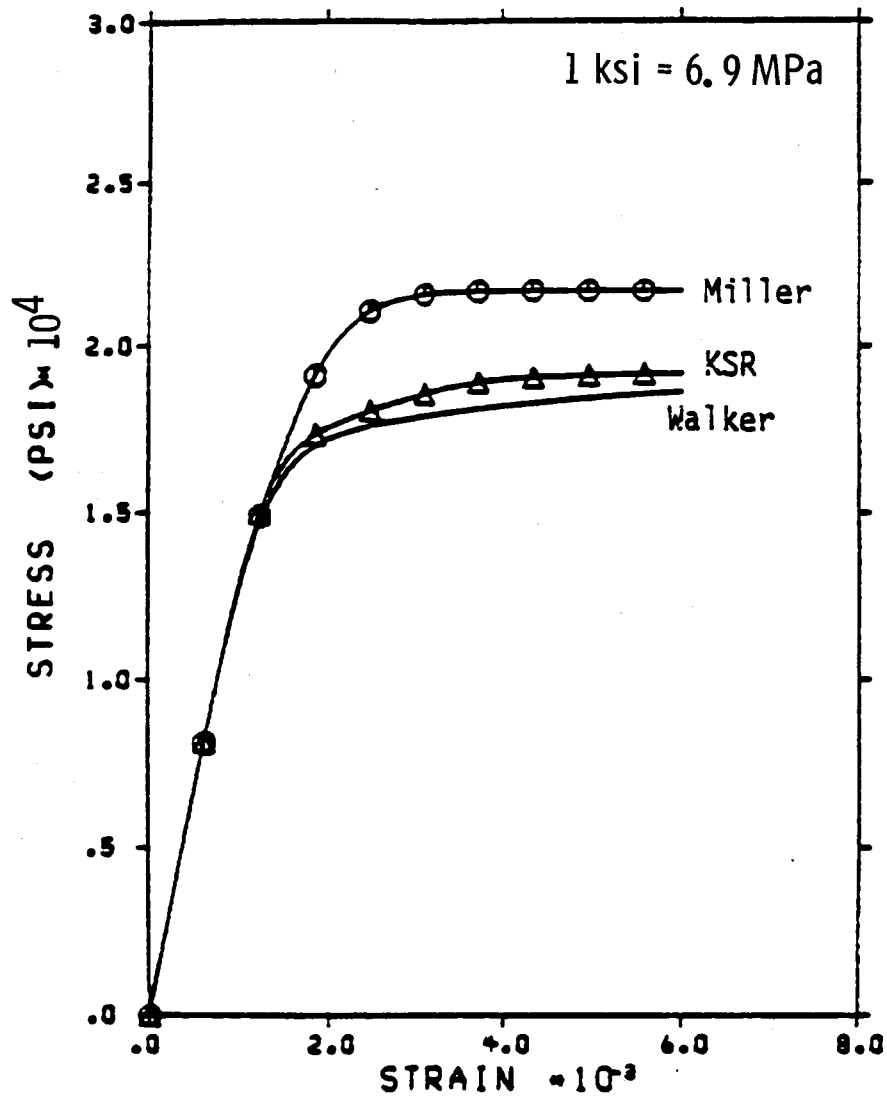


Figure 16. - Stress-strain response of Hastelloy-X: $T = 1800^{\circ} F (982^{\circ} C)$, $\dot{\epsilon} = 3.87 \times 10^{-3}/\text{sec}$.

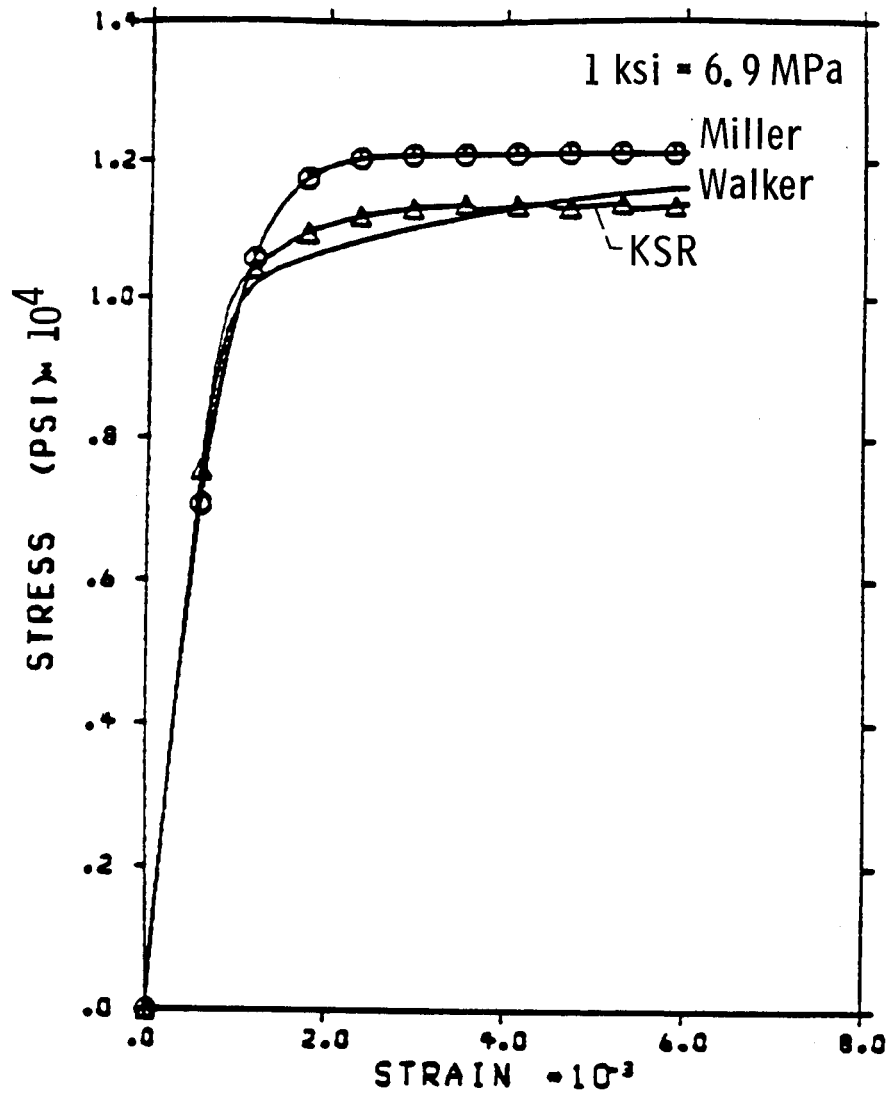


Figure 17. - Stress-strain response of Hastelloy-X: $T = 1800^{\circ} F (982^{\circ} C)$, $\dot{\epsilon} = 3.66 \times 10^{-4}/\text{sec}$.

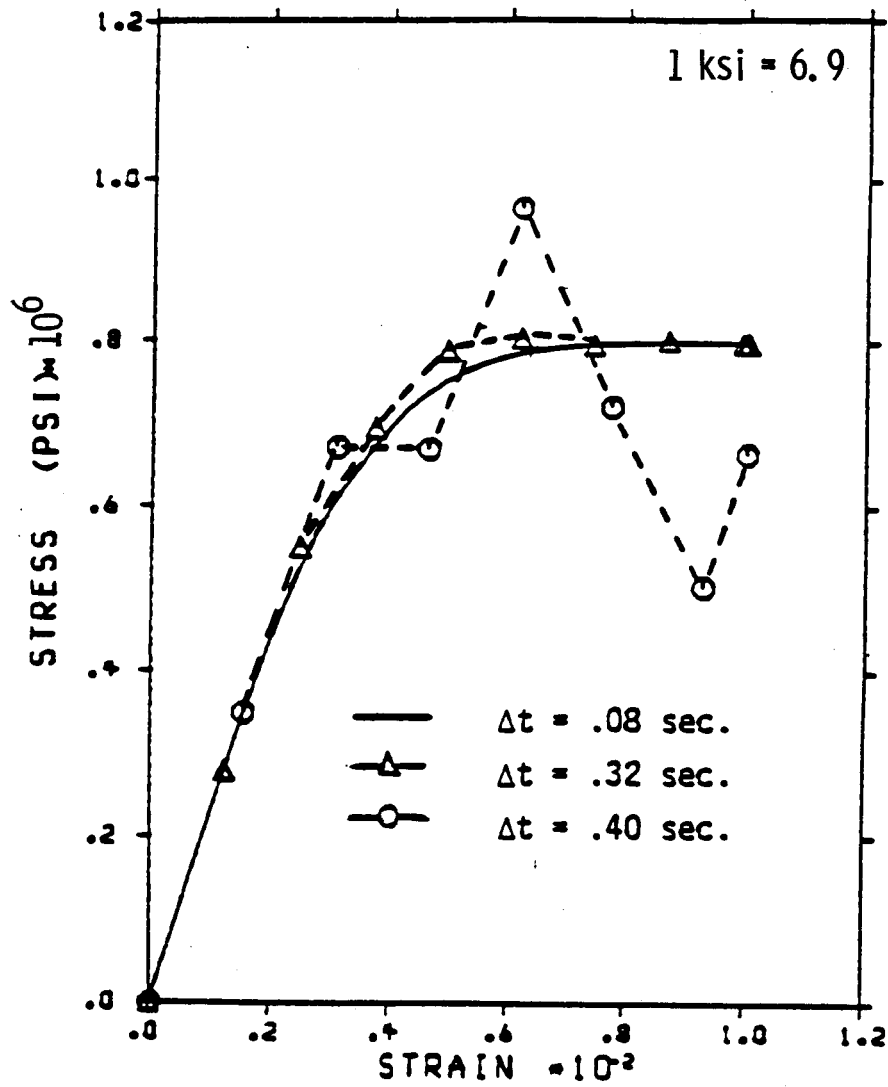


Figure 18. - Comparison of step sizes using forward Euler method: Walker's model
 $T = 1400^{\circ} \text{ F } (760^{\circ} \text{ C}), \dot{\epsilon} = 3.87 \times 10^{-3}/\text{sec.}$

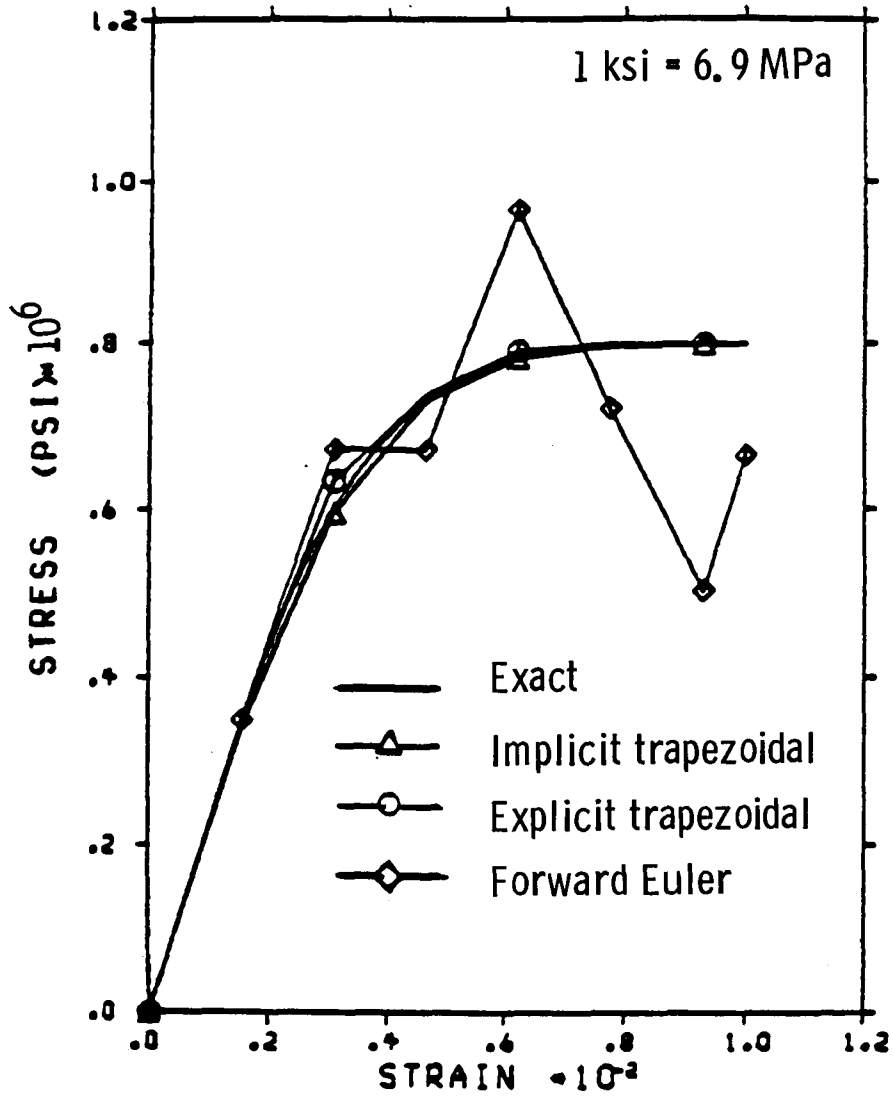


Figure 19. - Comparison of different integration schemes: forward Euler, explicit and implicit trapezoidal methods.

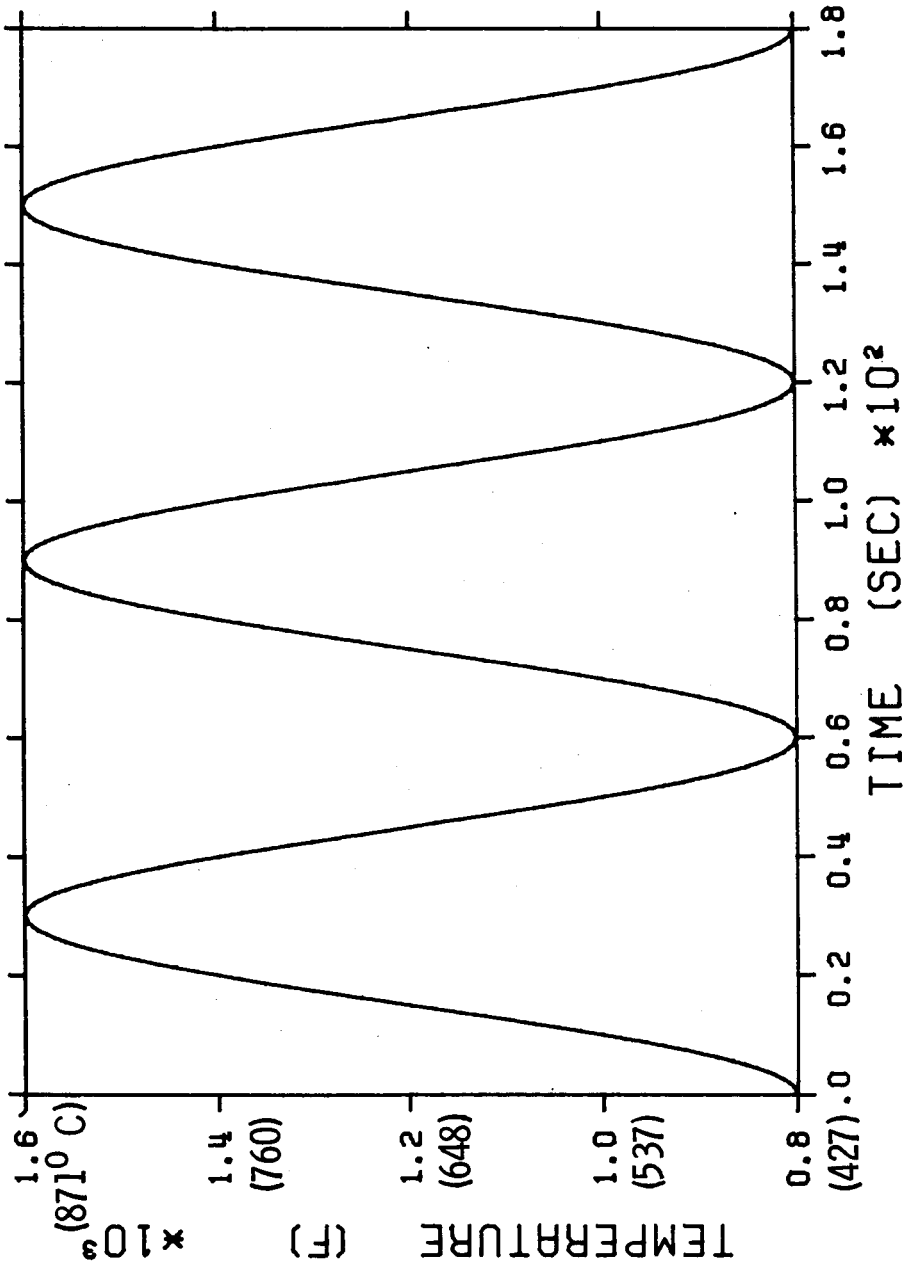


Figure 20. - Temperature history for closed symmetric loop.

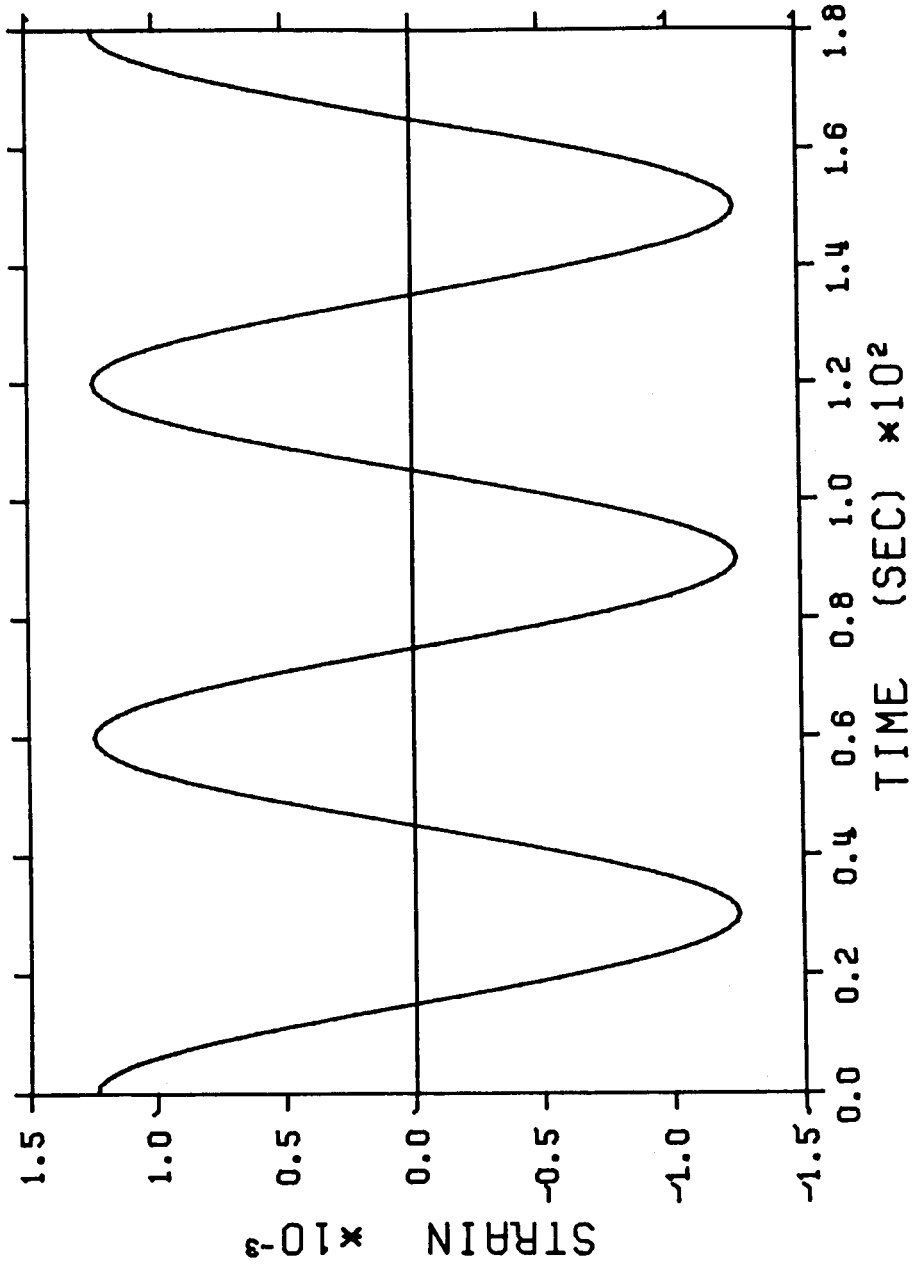


Figure 21. - Strain history for closed symmetric loop.

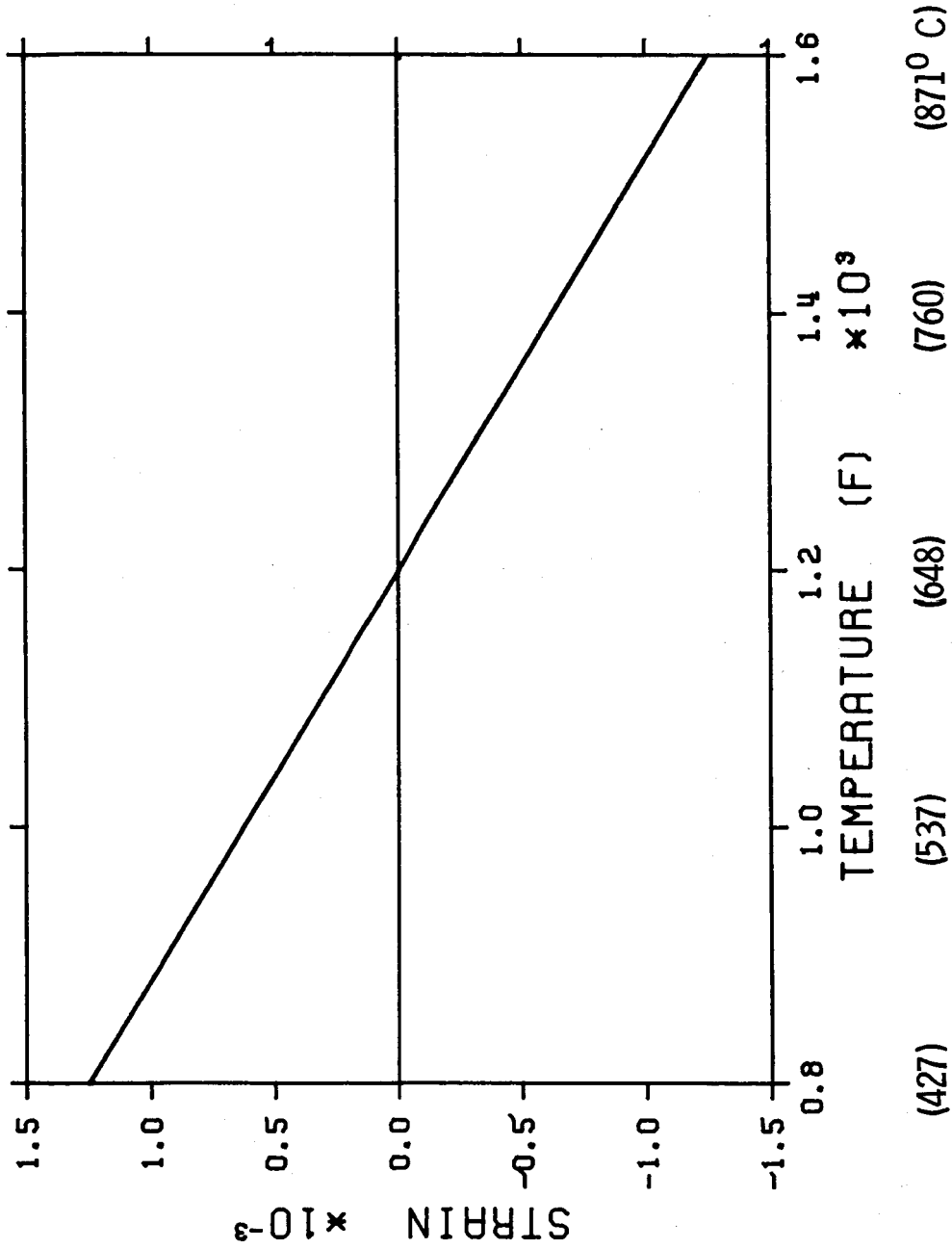


Figure 22. - Strain-temperature history for closed symmetric loop.

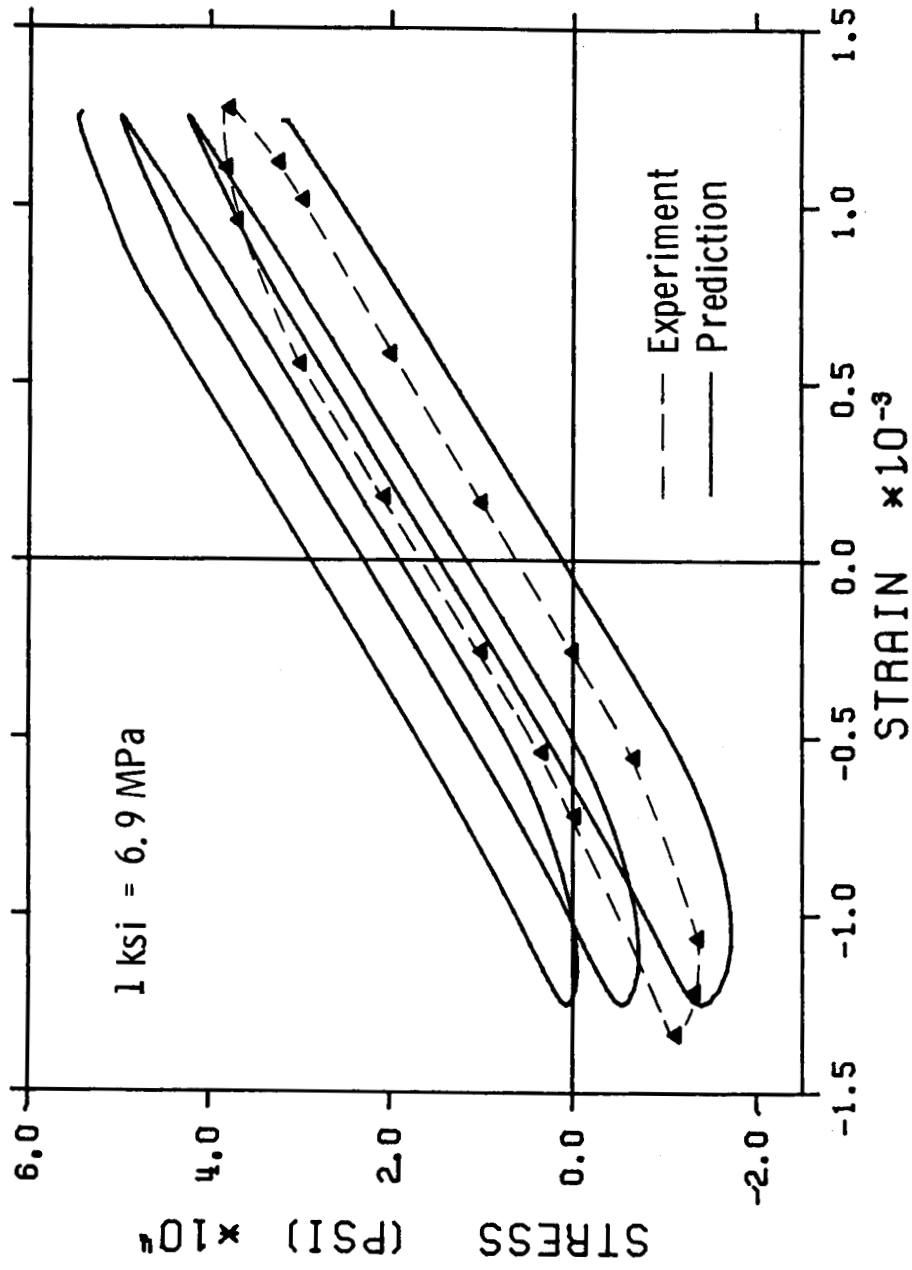


Figure 23. - Predicted response using Walker's model in comparison with experimental result for closed symmetric loop.

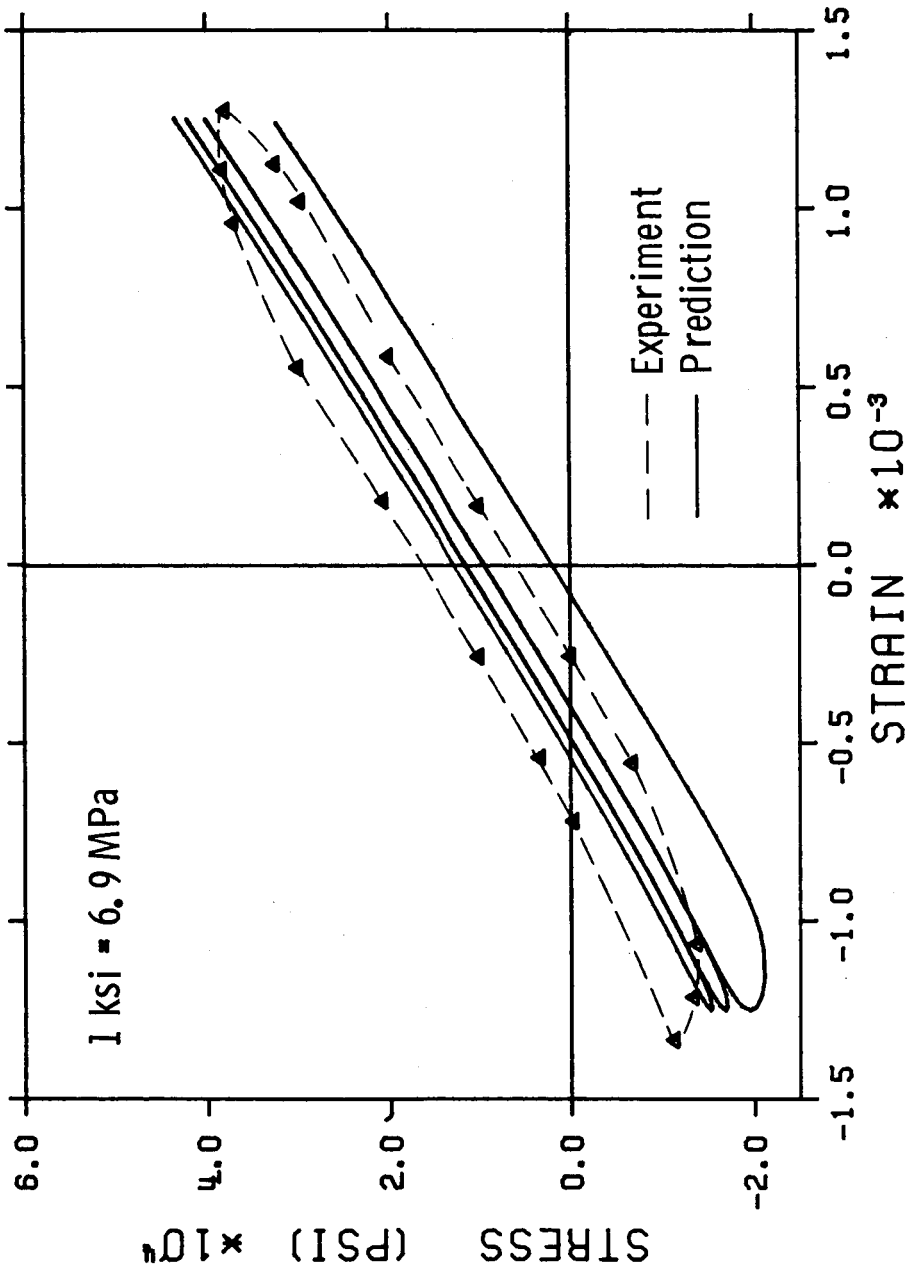


Figure 24. - Predicted responses using Miller's model in comparison with experimental result for closed symmetric loop.

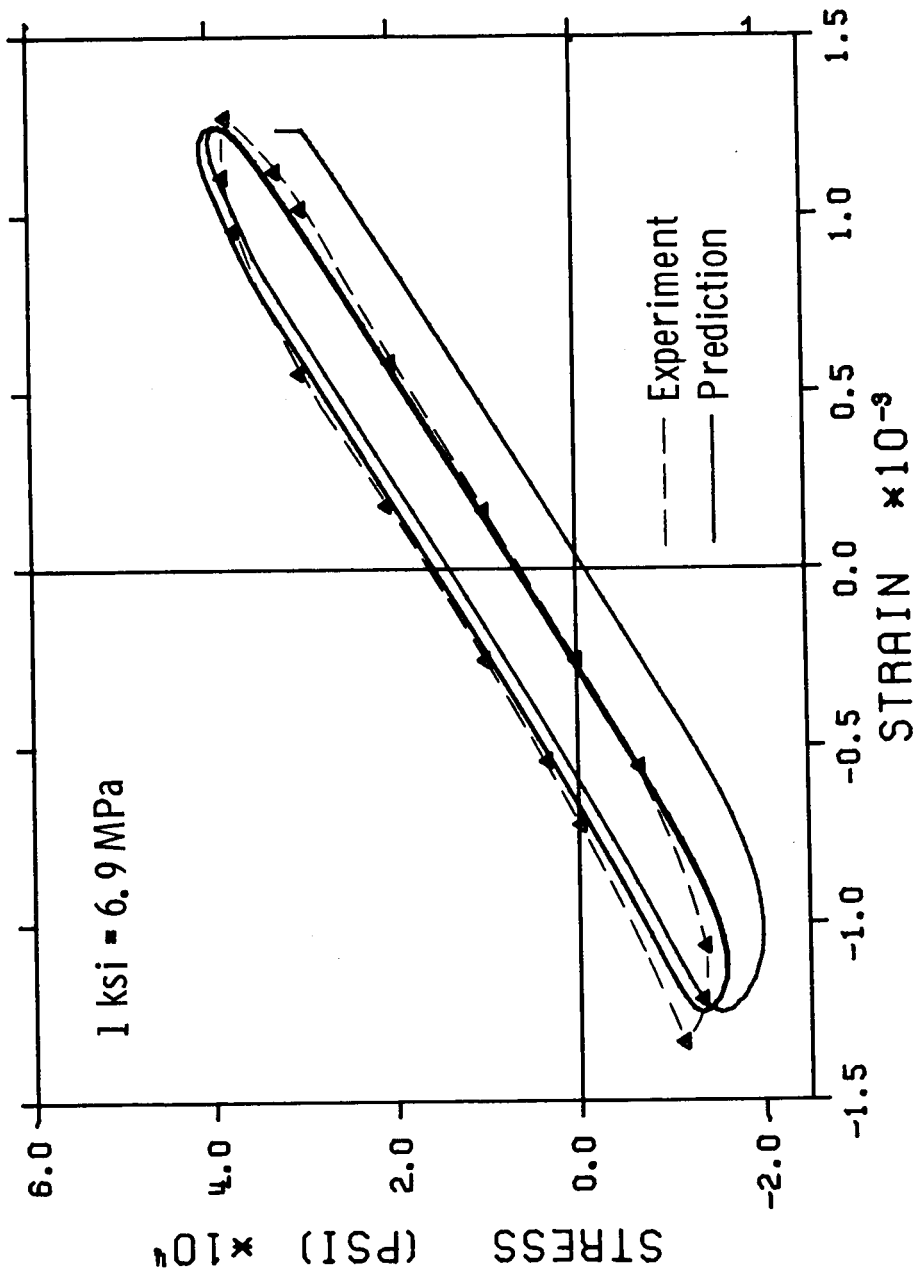


Figure 25. - Predicted responses using KSR's model in comparison with experimental result for closed symmetric loop.

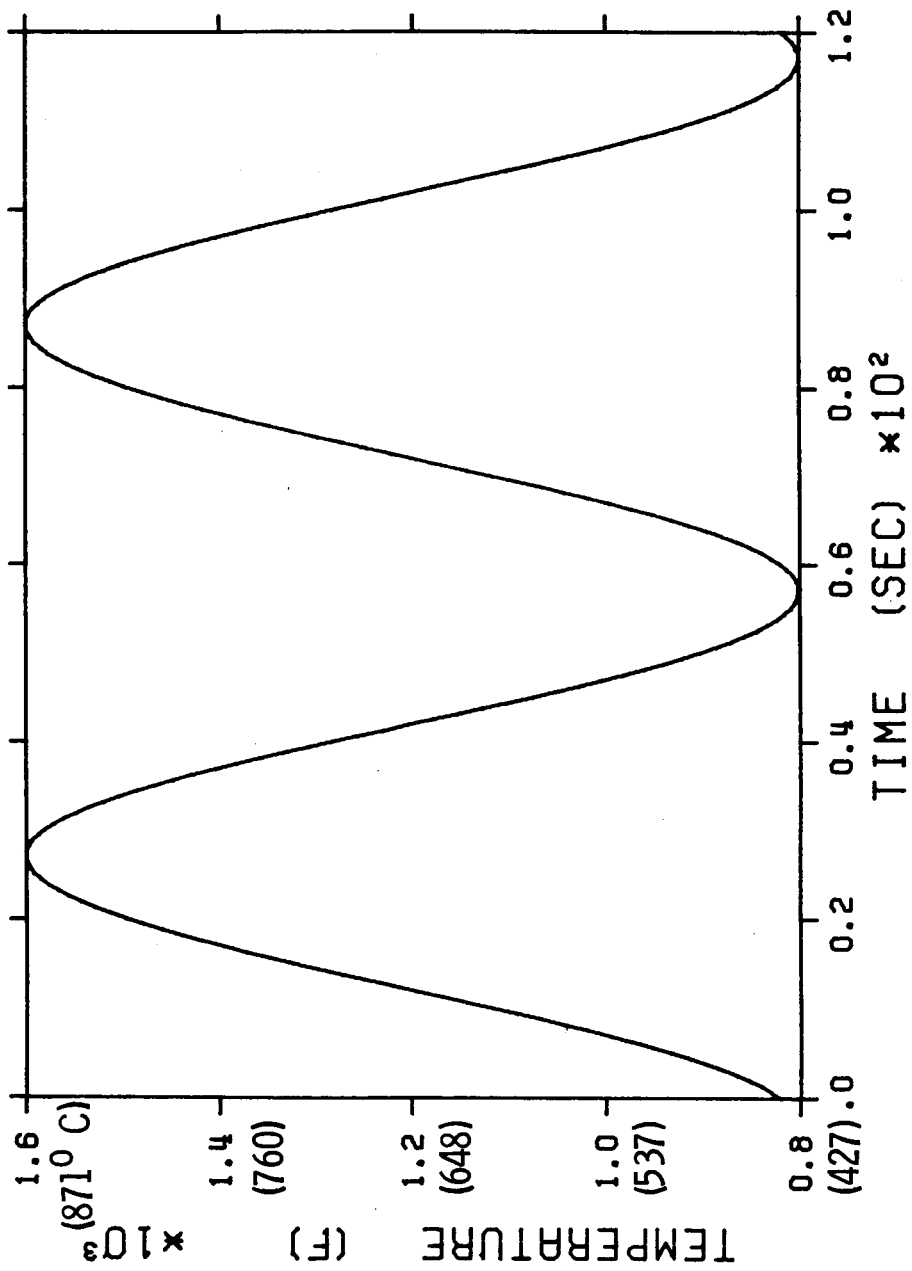


Figure 26. - Temperature history for open symmetrical loop.

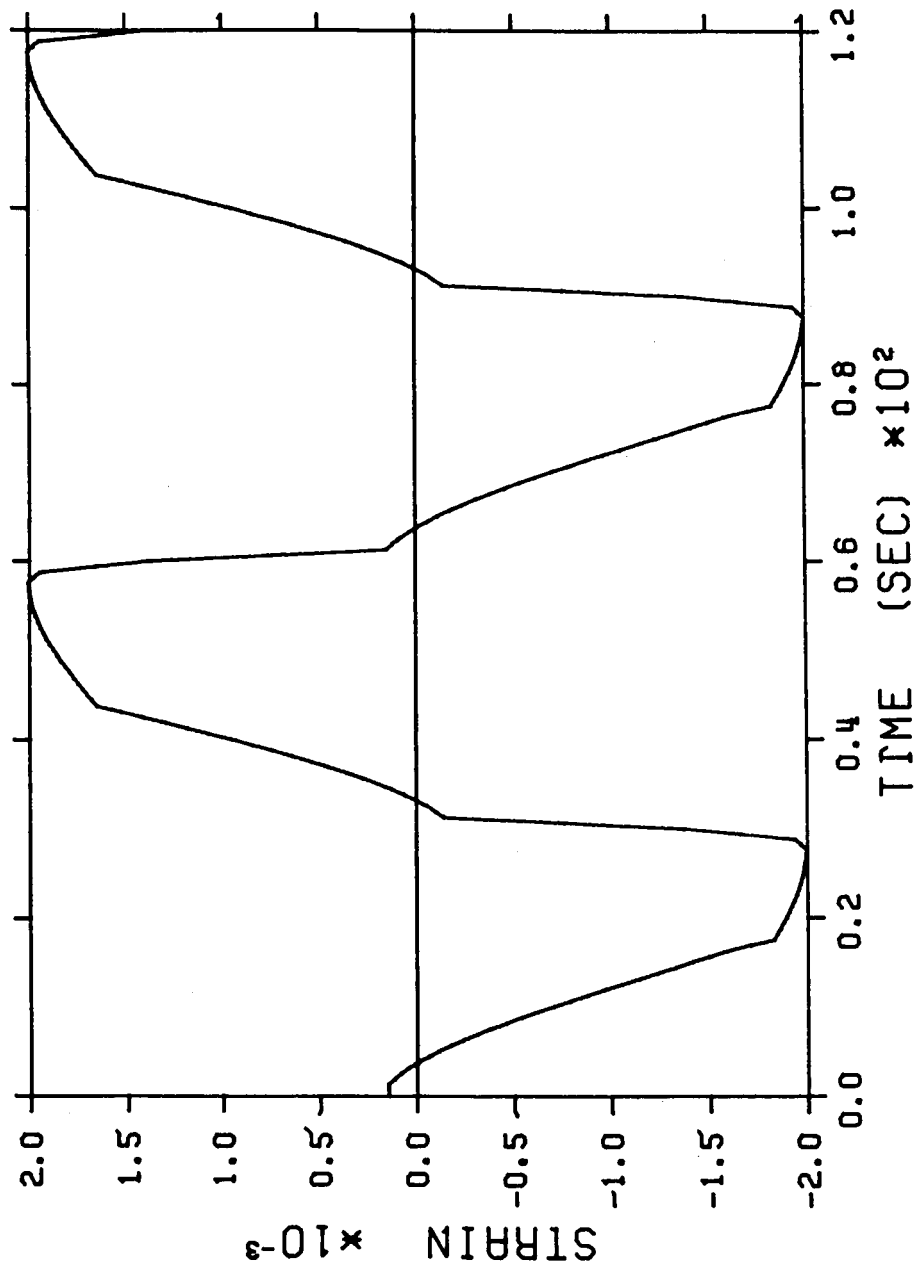


Figure 27. - Strain history for open symmetric loop.

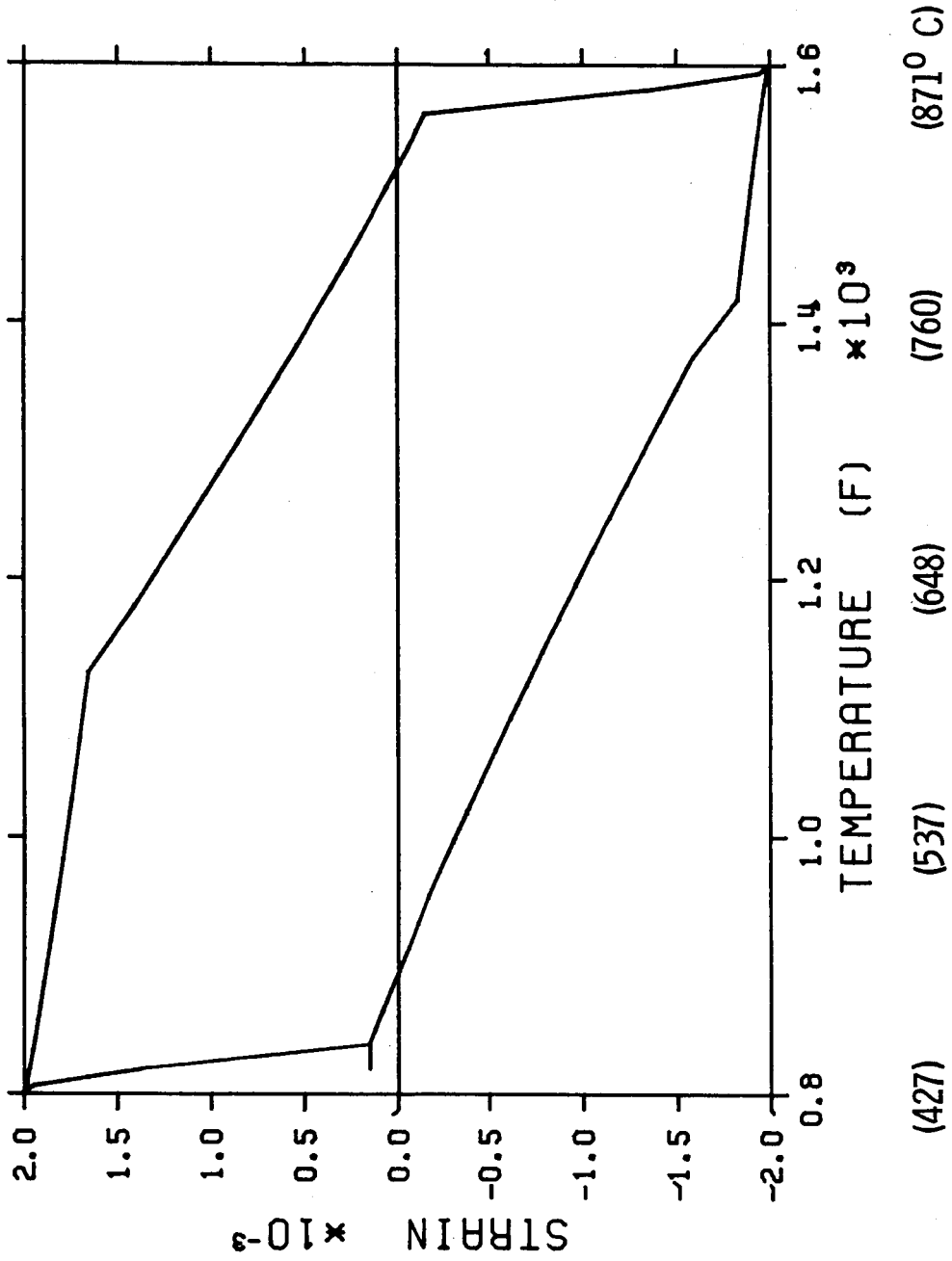


Figure 28. - Strain-temperature history for open symmetric history.

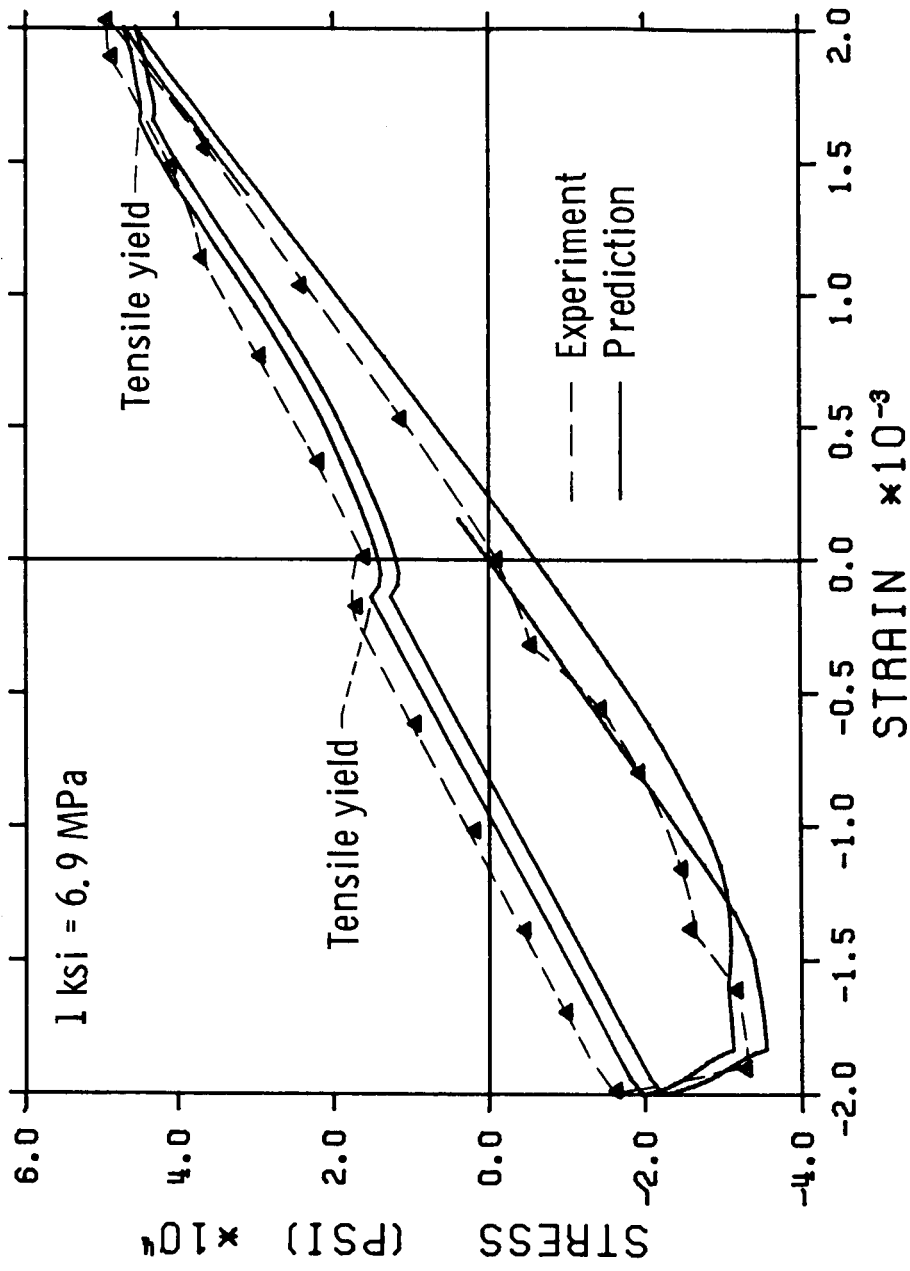


Figure 29. - Predicted response using Walker's model in comparison with experimental result for open symmetric loop.

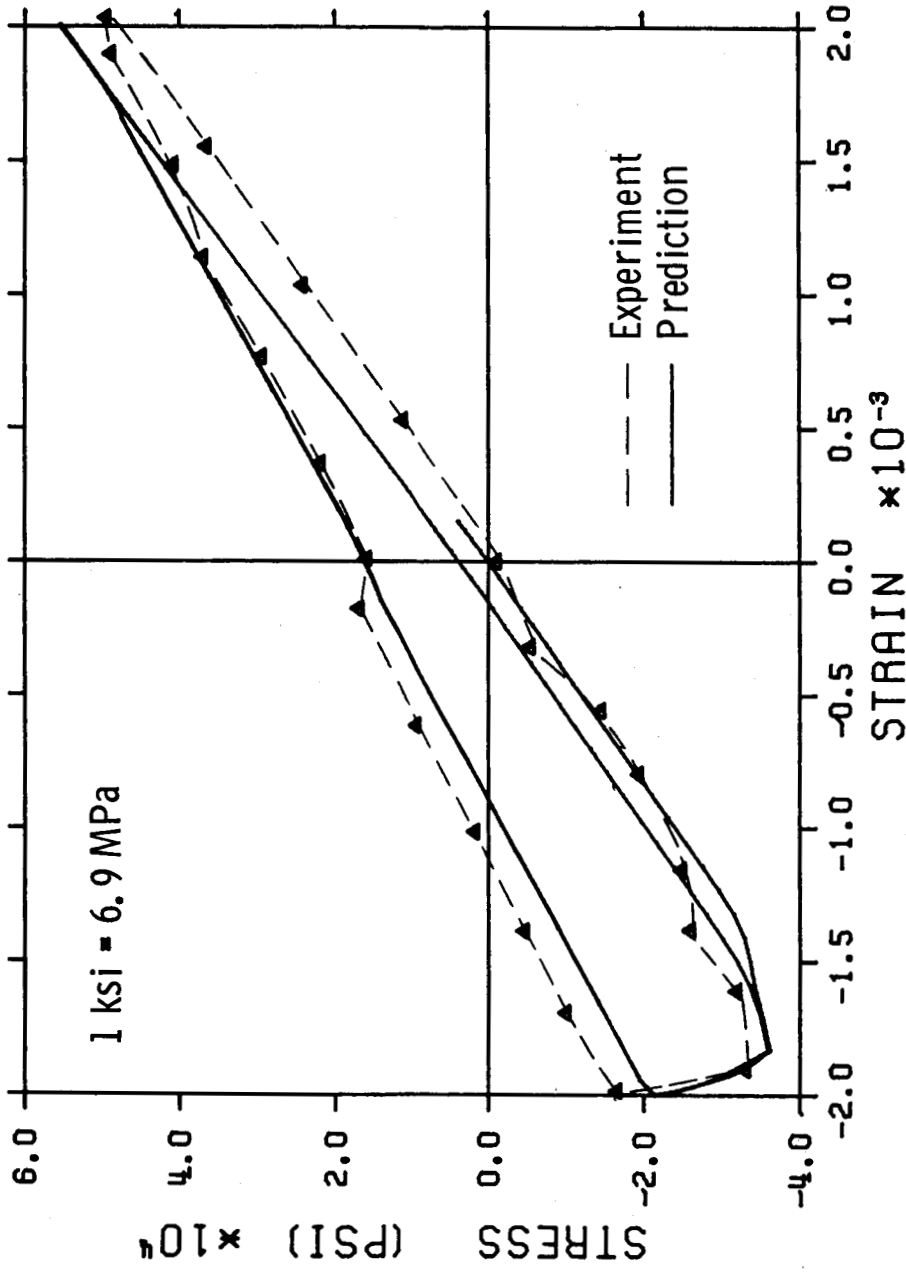


Figure 30. - Predicted response using Miller's model in comparison with experimental result for open symmetric loop.

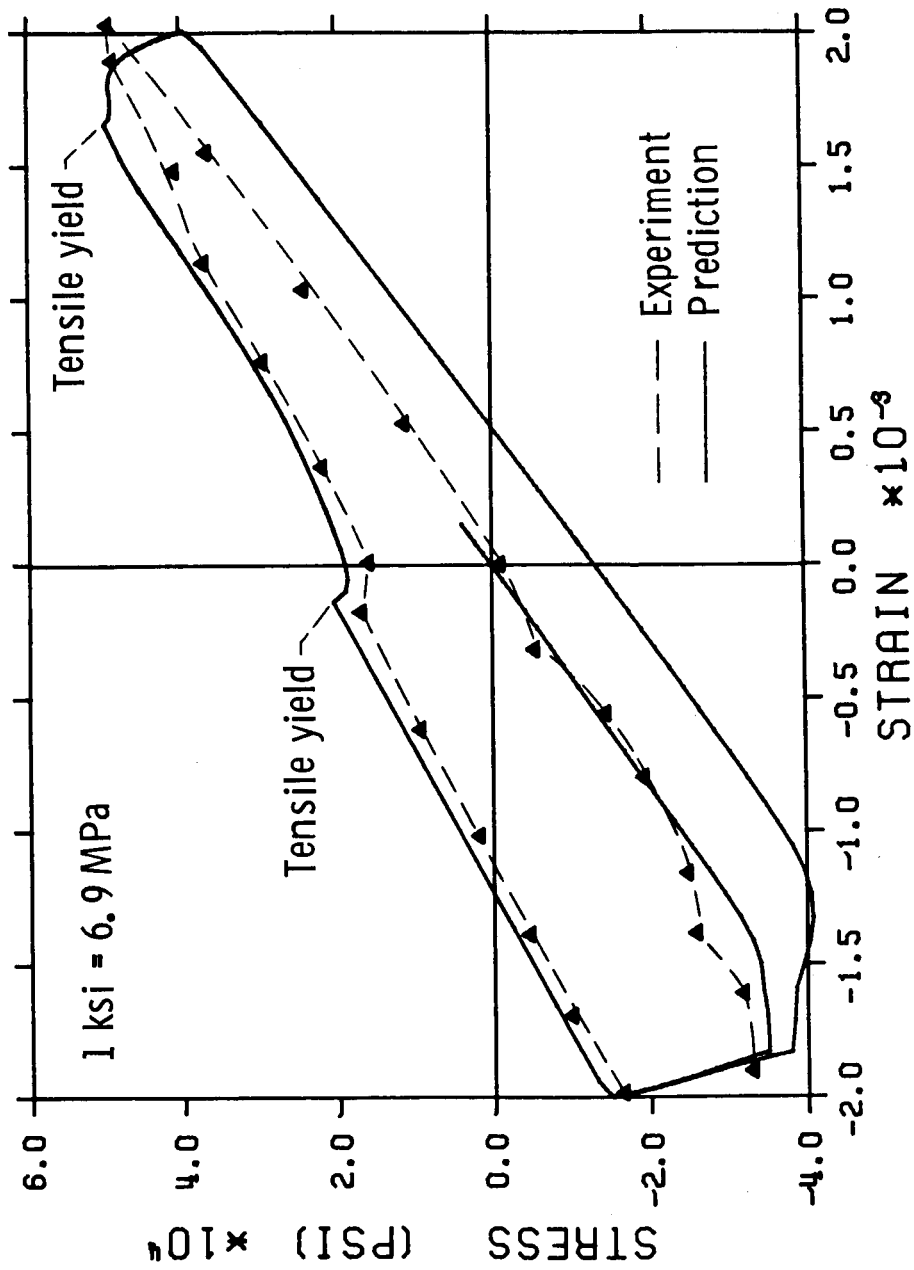


Figure 31. - Predicted response using KSR's model in comparison with experimental result for open symmetric loop.

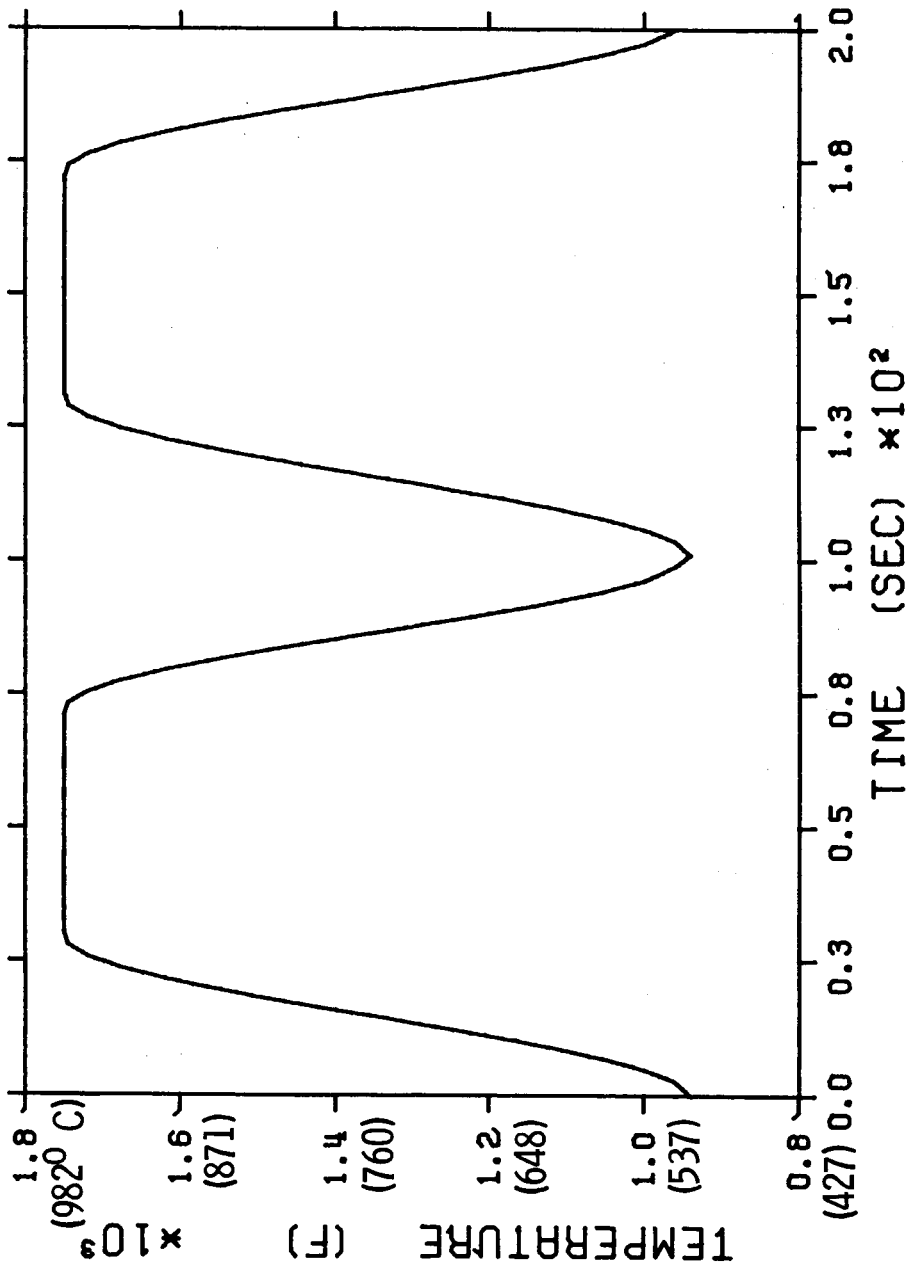


Figure 32. Temperature history for open non-symmetric loop.

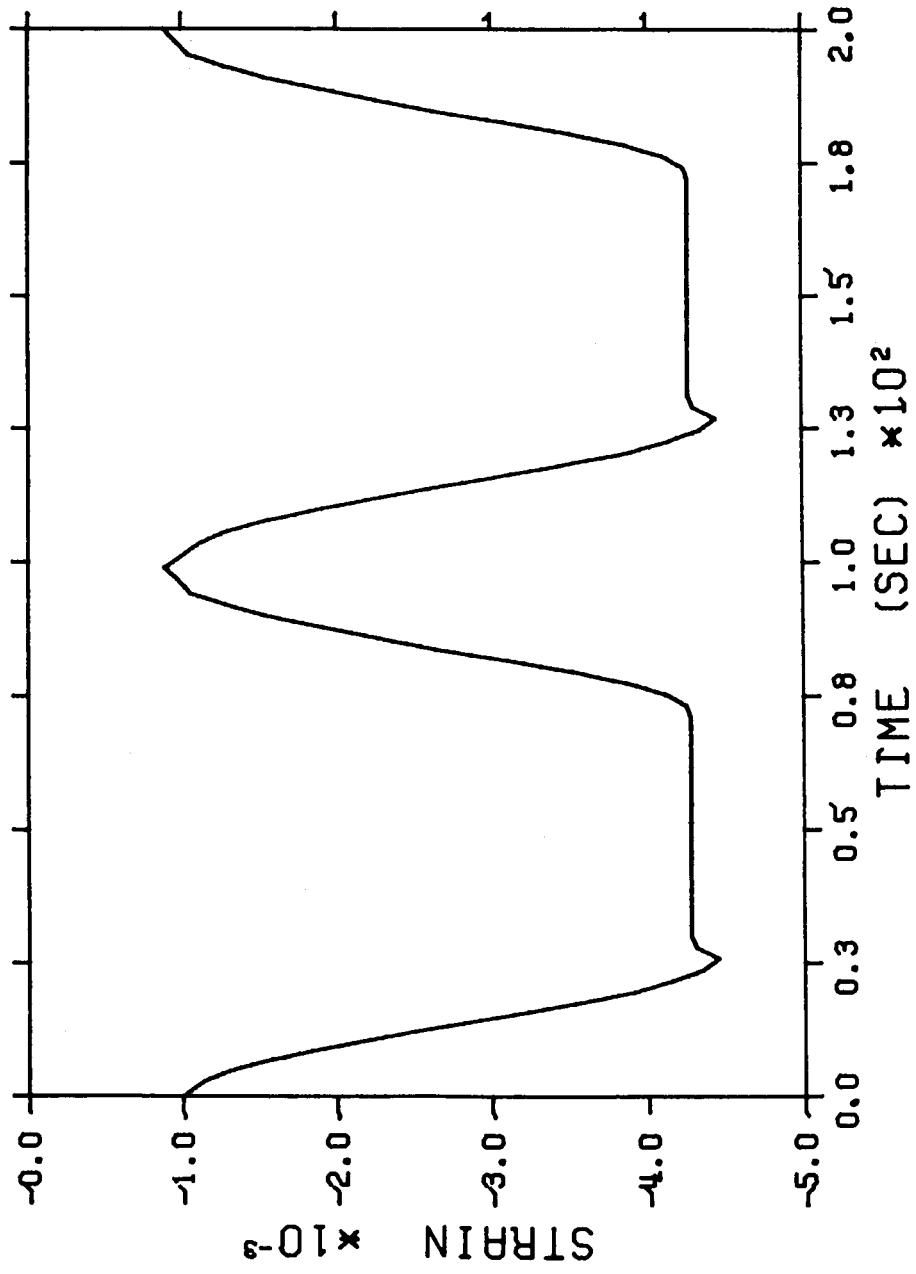


Figure 33. - Strain history for open non-symmetric loop.

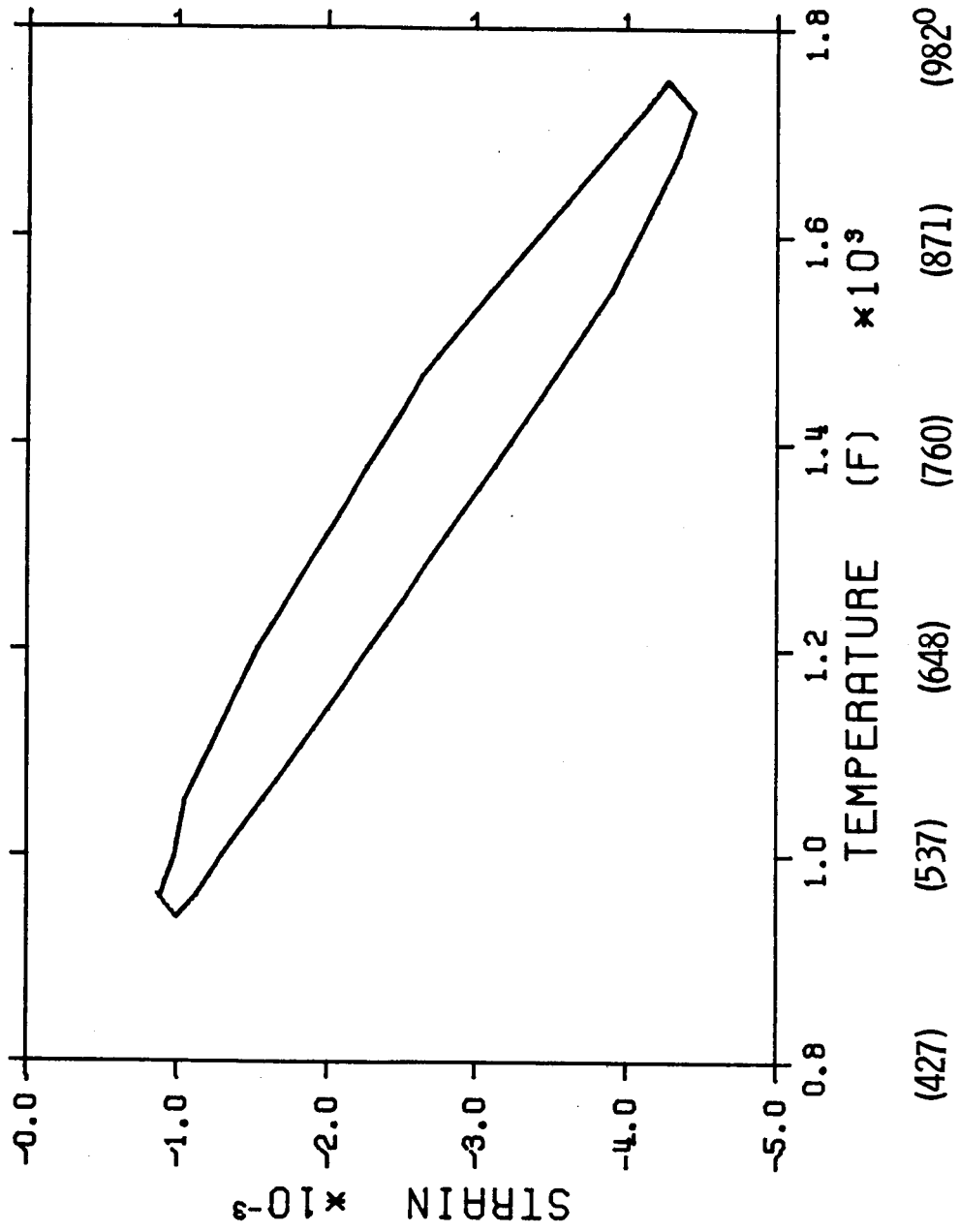


Figure 34. - Strain-temperature history for open non-symmetric loop.

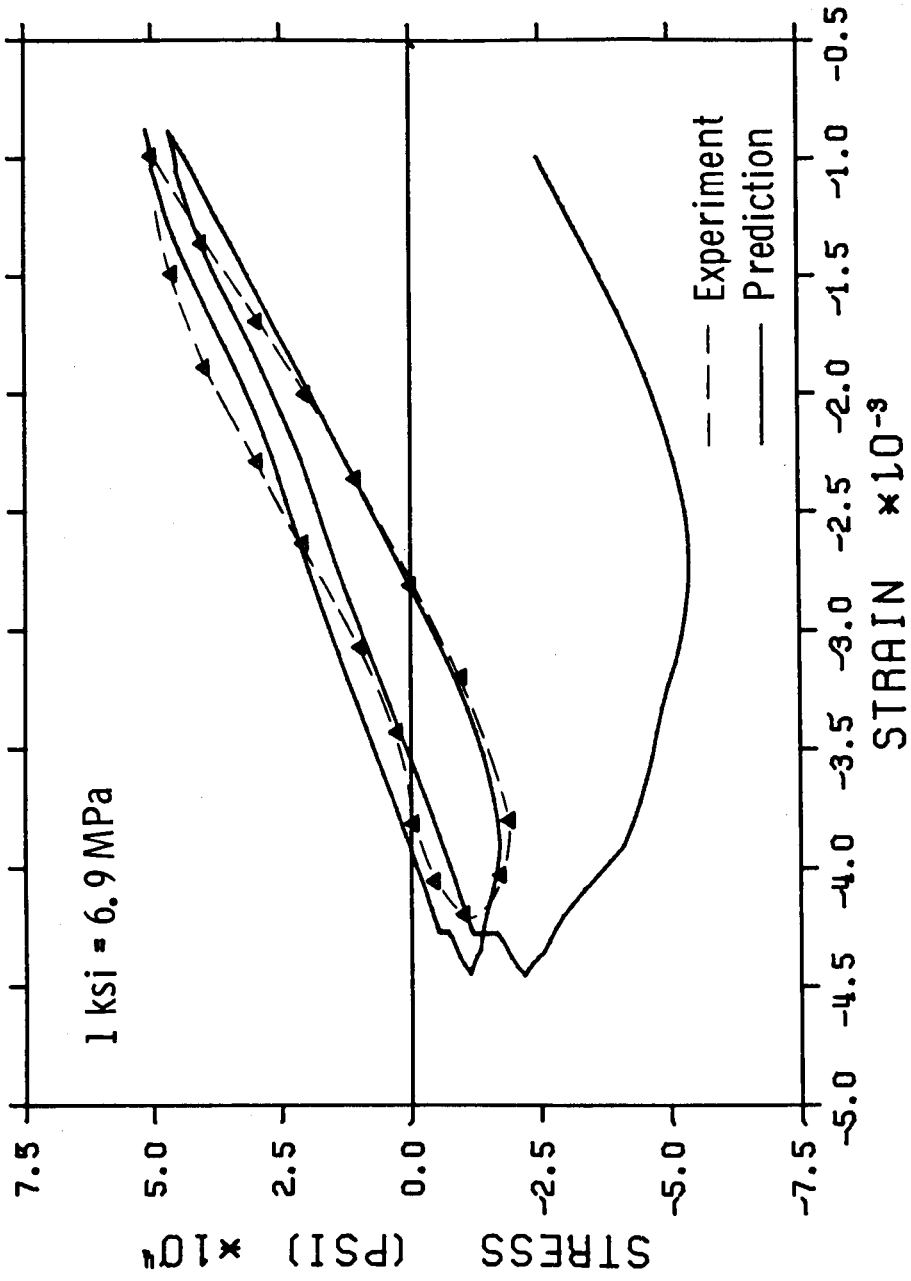


Figure 35. - Predicted response using Walker's model in comparison with experimental result for open non-symmetric loop.

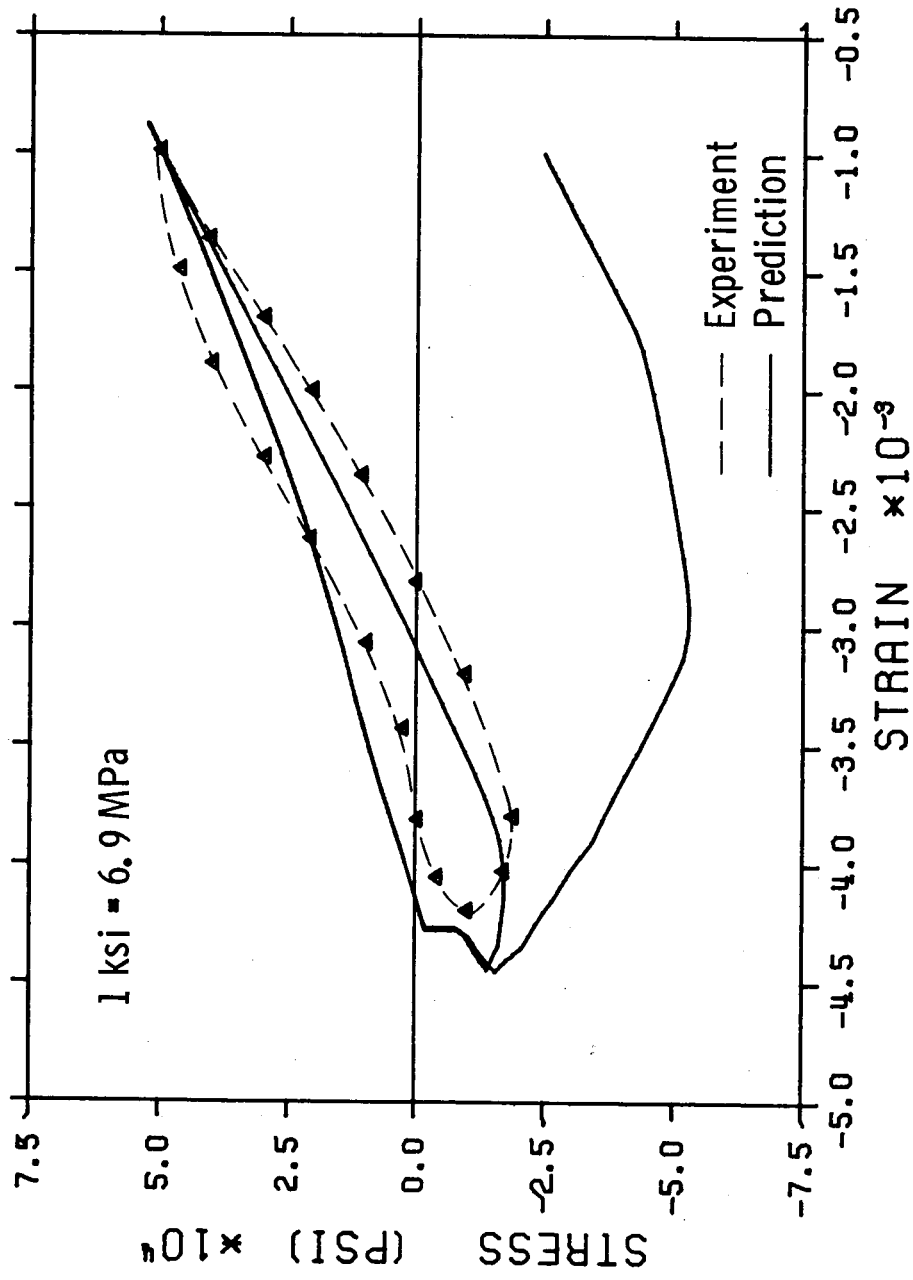


Figure 36. - Predicted response using Miller's model in comparison with experimental result for open non-symmetric loop.

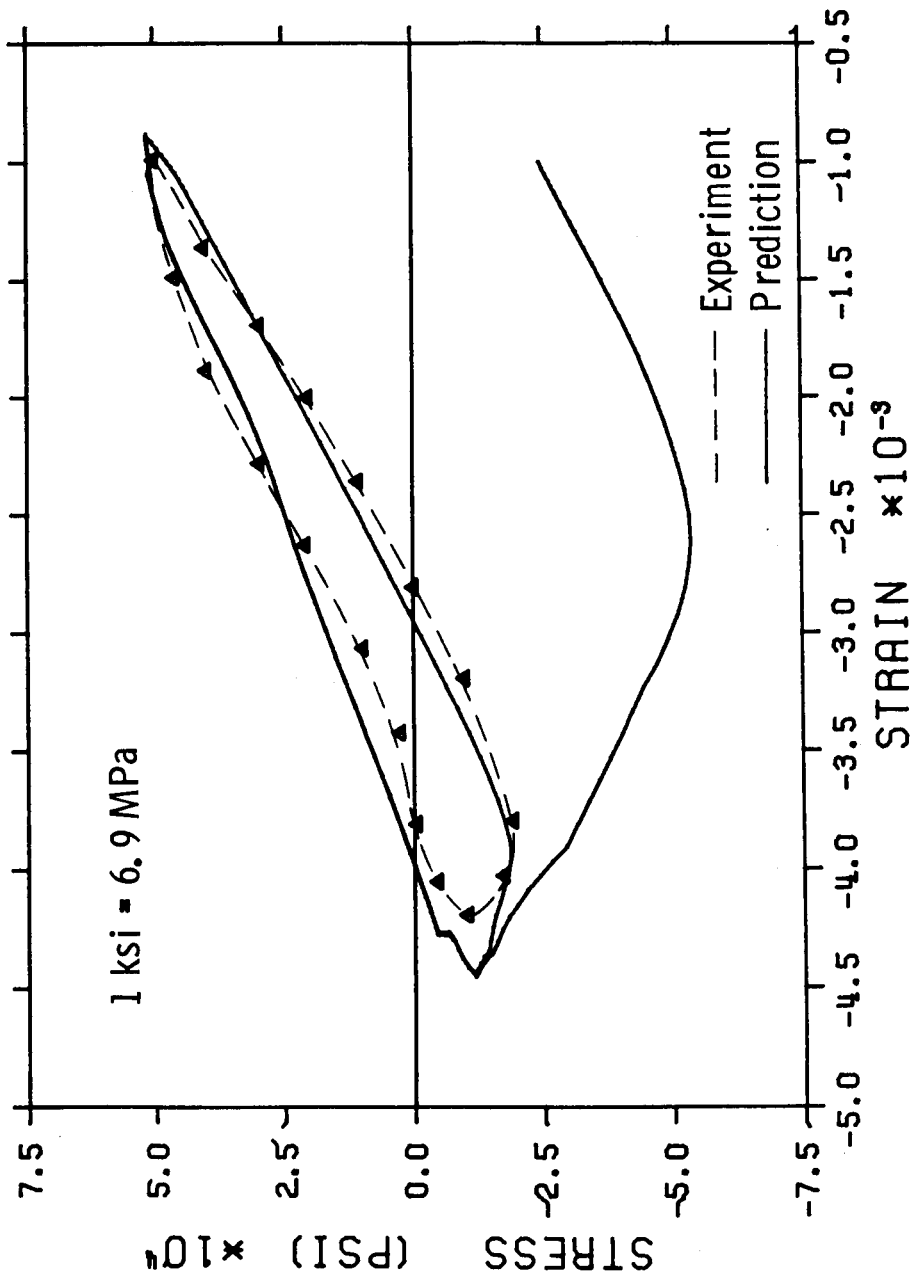


Figure 37. - Predicted response using KSR's model in comparison with experimental result for open non-symmetric loop.

1. Report No. NASA TM-83675		2. Government Accession No.		3. Recipient's Catalog No.	
4. Title and Subtitle A Computer Program For Predicting Nonlinear Uniaxial Material Responses Using Viscoplastic Models				5. Report Date July 1984	
				6. Performing Organization Code 533-04-1A	
7. Author(s) T. Y. Chang and R. L. Thompson				8. Performing Organization Report No. E-2120	
				10. Work Unit No.	
9. Performing Organization Name and Address National Aeronautics and Space Administration Lewis Research Center Cleveland, Ohio 44135				11. Contract or Grant No.	
				13. Type of Report and Period Covered Technical Memorandum	
12. Sponsoring Agency Name and Address National Aeronautics and Space Administration Washington, D.C. 20546				14. Sponsoring Agency Code	
15. Supplementary Notes T. Y. Chang, University of Akron, Akron, Ohio; R. L. Thompson, Lewis Research Center.					
16. Abstract A computer program was developed for predicting nonlinear uniaxial material responses using viscoplastic constitutive models. Four specific models, i.e., those due to Miller, Walker, Krieg-Swearengen-Rohde, and Robinson, are included in the present program. Any other unified model can be easily implemented into the program in the form of subroutines. Analysis features include stress-strain cycling, creep response, stress relaxation, thermomechanical fatigue loop, or any combination of these responses. In this report, an outline is given on the theoretical background of uniaxial constitutive models, analysis procedure, and numerical integration methods for solving the nonlinear constitutive equations. In addition, a discussion on the computer program implementation is also given. Finally, seven numerical examples are included to demonstrate the versatility of the computer program developed.					
17. Key Words (Suggested by Author(s)) Computer program; Nonlinear constitutive relations; Stress strain; Constitutive models			18. Distribution Statement Unclassified - unlimited STAR Category 39		
19. Security Classif. (of this report) Unclassified		20. Security Classif. (of this page) Unclassified		21. No. of pages	22. Price*